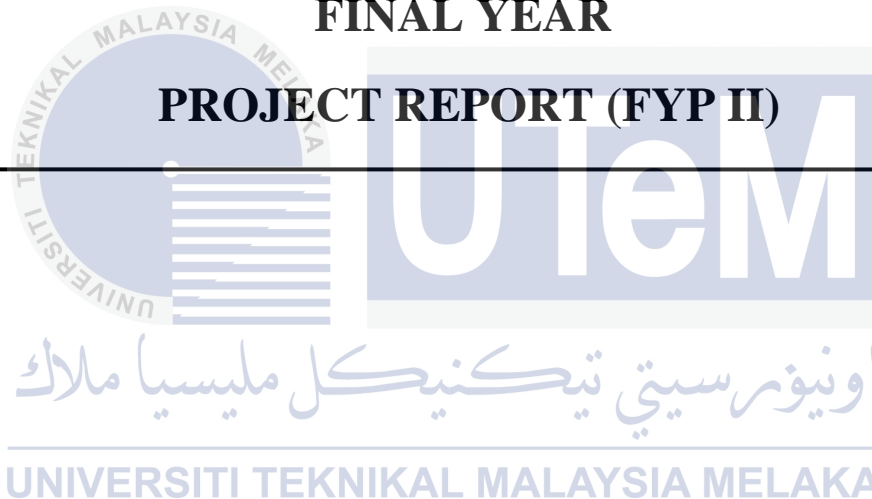




**FACULTY OF ELECTRICAL ENGINEERING
UNIVERSITI TEKNIKAL MALAYSIA MELAKA**

FINAL YEAR

PROJECT REPORT (FYP II)



**PMSM SENSORLESS CONTROL USING BACK-EMF BASED
POSITION AND SPEED ESTIMATION**

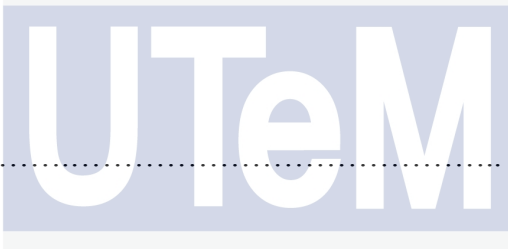
Muhammad Azfizan Bin Rahim

Bachelor of Electrical Engineering (Industrial Power)

Jun 2014

SUPERVISOR ENDORSEMENT

“I hereby declare that I have read through this report entitle “PMSM Sensorless Control Using Back-EMF Based Position and Speed Estimation” and found that it has comply the partial fulfillment for awarding the degree of Bachelor of Electrical Engineering (Industrial Power)”



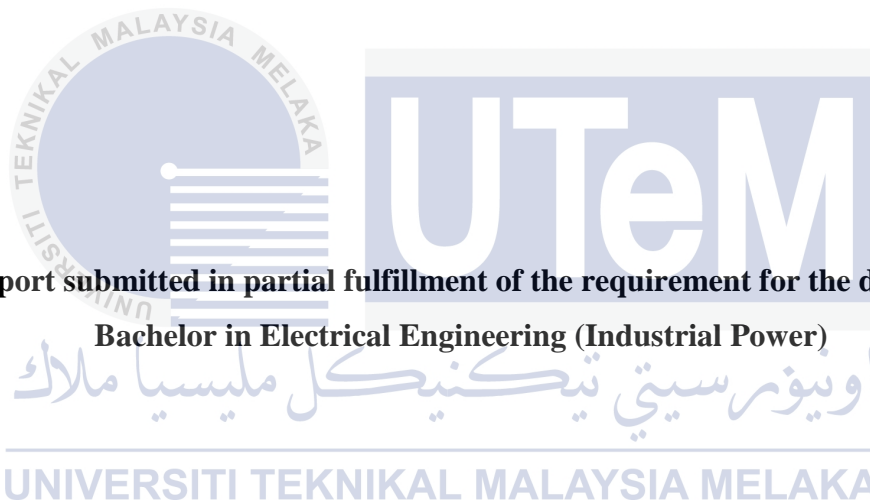
Signature :

Supervisor's Name :
اونيورسيتي تيكنيكل مليسيا ملاك

Date :
UNIVERSITI TEKNIKAL MALAYSIA MELAKA

**PMSM SENSORLESS CONTROL USING BACK-EMF BASED POSITION AND
SPEED ESTIMATION**

MUHAMMAD AZFIZAN BIN RAHIM

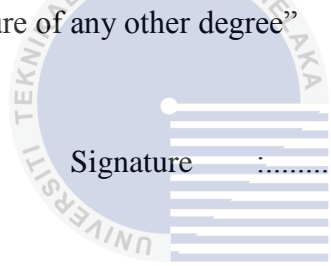


Faculty of Electrical Engineering

UNIVERSITI TEKNIKAL MALAYSIA MELAKA

2013/2014

“I declare this report entitle “PMSM Sensorless Control Using Back-EMF Based Position and Speed Estimation” is the result of my own research except as cited in the references. The report wasn’t accepted for any degree and is not concurrently submitted in the candidature of any other degree”



Signature :

Name : اونيورسيتي تيكنيكل مليسيا ملاك

Date : UNIVERSITI TEKNIKAL MALAYSIA MELAKA

ACKNOWLEDGEMENT

ALHAMDULILLAH, I am grateful to God for His blessing and mercy of the His to make this project successful and complete in this semester. First of all, I would like to express to Universiti Teknikal Malaysia Melaka (UTeM). The special thanks go to my helpful supervisor Pn. Jurifa Binti Mat Lazi for giving invaluable guidance supervision, committed and sustained with patience during this project. The supervision and support that she gave truly help the progression and smoothness in the Final Year Project. In addition, I also wish to express to all the people involved in this thesis either directly or indirectly, especially to the entire lecture who have taught me. Thank you for the lessons that have been taught.

My sincere thanks go to all my friends is the one same guidance under Pn. Jurifa Binti Mat Lazi, they are Muhammad Faiz Salim, Mohd Hafiz Hamit and Amirul Ikhsan Burhannudin because willing to support and gives some knowledge to achieve the aim of this final year project. Instead of that, special thanks that I gave to another supporter friends who sincerely give their opinion and continuous guidance throughout this Final Year Project program.

Not forgotten also, thanks to my family for their support and endless encouragement to successfully complete in this project.

ABSTRACT

This report presents the progress report on research for “PMSM Sensorless Control Using Back-EMF Based Position and Speed Estimation”. The objectives is to model and simulate a position and speed estimator based on back-EMF sensorless control on PMSM and to analyze the performance of sensorless operation related to the back-EMF of the PMSM. These motor drives are very essential for industrial applications. In the applications of PMSM drive, the rotor position signal is obtained from a mechanical sensor that will reduce the reliability of the system and added the cost of the drives. Therefore, a strong desire arises in the alternative of PMSM sensorless control, where the estimators are employed to provide the feedback data required by the control system. Because of that, the development position and speed estimation based on back-EMF sensorless control for PMSM is performed. The performance of the back-EMF based sensorless vector control is mainly determined by the sensorless algorithms to relate to the position and speed estimation. The appropriate controller use in this project such as vector control, hysteresis current controller and PI controller. In this project, sensorless control approach using back-EMF method. The overall system is simulated by using SIMULINK/MATLAB software. This case study presents a position and speed estimation method based on back-EMF sensorless control by measuring the phase currents and voltages of the PMSM drive estimator to get the exact position and speed estimator. On the other hand, the sensorless control method provides satisfactory efficiency when use in PMSM drive.

ABSTRAK

Laporan ini membentangkan pelaksanaan laporan penyelidikan untuk "PMSM Tanpa Pengesan Kawalan Menggunakan Balikan-EMF Berdasarkan Anggaran Kedudukan Dan Kelajuan". Objektifnya adalah untuk memodelkan dan mensimulasikan kedudukan dan kelajuan penganggar berdasarkan balikan-EMF kawalan tanpa pengesan pada PMSM dan untuk menganalisis prestasi operasi tanpa pengesan berkaitan dengan balikan-EMF daripada PMSM. Pemacu motor adalah sangat penting bagi kegunaan industri. Dalam aplikasi pemacu PMSM, isyarat kedudukan pemutar diperolehi daripada pengesan mekanikal yang akan mengurangkan kebolehpercayaan sistem dan menambahkan kos pemacu. Oleh itu, keinginan yang kuat timbul dalam alternatif kawalan tanpa pengesan pada PMSM, di mana penganggar digunakan untuk menyediakan data-data maklum balas yang diperlukan oleh sistem kawalan. Oleh kerana itu, kedudukan dan kelajuan anggaran dibangunkan berdasarkan kawalan balikan-EMF tanpa pengesan untuk PMSM dilakukan. Prestasi daripada balikan-EMF tanpa pengesan berasaskan kawalan vektor ditentukan terutamanya oleh algoritma tanpa pengesan berkaitan dengan anggaran kedudukan dan kelajuan. Penggunaan pengawalan yang sesuai digunakan di dalam projek ini adalah seperti kawalan vektor, kawalan arus histerisis dan pengawalan PI. Di dalam projek ini, pendekatan kawalan tanpa pengesan yang menggunakan kaedah balikan-EMF. Keseluruhan sistem adalah disimulasikan dengan menggunakan perisian SIMULINK / MATLAB. Kajian kes ini membentangkan kaedah anggaran kedudukan dan kelajuan berdasarkan kawalan tanpa pengesan pada balikan-EMF dengan langkah mengukur arus fasa dan voltan pada penganggar PMSM untuk mendapatkan kedudukan dan kelajuan penganggar yang tepat. Sementara itu, kaedah kawalan tanpa pengesan menyediakan kecekapan yang memuaskan apabila digunakan di dalam PMSM.

TABLE OF CONTENTS

CHAPTER	TITLE	PAGE
	ACKNOWLEDGEMENT	iv
	ABSTRACT	v
	TABLE OF CONTENTS	vii
	LIST OF TABLES	ix
	LIST OF FIGURES	x
	LIST OF ABBREVIATIONS	xiii
	LIST OF SYMBOLS	xiv
	LIST OF APPENDICES	xv
1	INTRODUCTION	1
	1.1 Introduction	1
	1.2 Motivation	2
	1.3 Problem Statement	2
	1.4 Objective	3
	1.5 Project Scope	3
	1.6 Project Outline	3
2	LITERATURE REVIEW	4
	2.1 Theory and Basic Principles	4
	2.1.1 Permanent Magnet Synchronous Machine (PMSM)	4
	2.1.2 Field Oriented Control (FOC)	7
	2.1.3 Proportional Integral (PI) Controller	9
	2.1.4 Space Vector	9

CHAPTER	TITLE	PAGE
	2.1.5 Space Vector Pulse Width Modulation (SVPWM)	14
	2.1.6 Position and Speed Estimator Of FOC	18
	2.1.7 Back-EMF Using Sensorless Control	19
	2.2 Comparison with other method of sensorless	22
	2.3 Previous Related Works	22
	2.3.1 Summary Of The Review	25
3	METHODOLOGY	27
	3.1 Introduction	27
	3.2 Overall Process Flow Chart	28
	3.2.1 Description Of Flow Chart	29
	3.3 Project Phase	31
4	RESULT AND DISCUSSION	39
	4.1 Introduction	39
	4.2 Simulation of PMSM Using Back-EMF Sensorless Control	39
	4.3 Back-EMF Observer	42
	4.4 Result Of Simulation	42
	4.4.1 Simulation without load disturbance condition	43
	4.4.2 Simulation with load disturbance condition	53
	4.5 Analysis	62
5	CONCLUSION AND RECOMMENDATIONS	65
	5.1 Conclusion	65
	5.2 Recommendations	66
	REFERENCES	67
	APPENDICES	69

LIST OF TABLES

TABLE	TITLE	PAGE
2.1	Eight on-off states of the inverter	17
2.2	Comparison other method	22
2.3	Summary of the previous related work	26
4.1	Parameter of induction motor	41
4.2	Simulation result of reference speed with step-up response	62
4.3	Simulation result of reference speed with load disturbance	62



اونيورسيتي تيكنيكل مليسيا ملاك

UNIVERSITI TEKNIKAL MALAYSIA MELAKA

LIST OF FIGURES

FIGURE	TITLE	PAGE
2.1	Basic block diagram of PMSM	5
2.2	Equivalent circuit of the PMSM	6
2.3	Basic scheme of FOC for AC motor	8
2.4	Stator current space vector and its component in (a, b, c)	10
2.5	Clarke transformation using reference frame	11
2.6	Stator current space vector and its component in (a, b) and in the d, q rotating reference frame	12
2.7	Topology of a three-leg voltage source inverter	15
2.8	Voltage waveforms of a three-phase VSI	15
2.9	Eight switching state topologies of a voltage source inverter	16
2.10	Diagram of voltage space vector	17
2.11	Block diagram of the position and speed estimation method	18
2.12	Phasor diagram of PMSM	21
3.1	Overall project process	28
3.2	Flow of phase project	31
3.3	Block diagram of the basic motor with estimator	32
3.4	Block diagram of the position and speed estimation method	33
3.5	PI controller block	34
3.6	Inverse park transformation block	34
3.7	SVPWM block	35
3.8	Clarke transformation block	36
3.9	Park transformation block	36
3.10	Back-EMF estimator block	37
4.1	Overall simulation block diagram of PMSM using back-EMF sensorless control system	40
4.2	Estimator block diagram in simulation	42

FIGURE	TITLE	PAGE
4.3	Comparison between reference speed, speed estimator and actual speed	43
4.4	Zoom view at starting speed during forward condition	44
4.5	Zoom view at starting speed during reverse condition	44
4.6	Comparison between actual position and position estimator of rotor	45
4.7	Comparison between current I_a , I_b and I_c	45
4.8	Zoom view during the starting current	46
4.9	Comparison between reference speed, speed estimator and actual speed	46
4.10	Zoom view at starting speed during forward condition	47
4.11	Zoom view at starting speed during reverse condition	47
4.12	Comparison between actual position and position estimator of rotor	48
4.13	Comparison between current I_a , I_b and I_c	48
4.14	Zoom view during the starting current	49
4.15	Comparison between reference speed, speed estimator and actual speed	49
4.16	Zoom view at starting speed during forward condition	50
4.17	Zoom view at starting speed during reverse condition	50
4.18	Comparison between actual position and position estimator of rotor	51
4.19	Comparison between current I_a , I_b and I_c	51
4.20	Zoom view during the starting current	52
4.21	Graph comparison between reference speed, speed estimator and actual speed with load disturbance	53
4.22	Zoom view of speed during load disturbance	53
4.23	Comparison between actual position and position estimator of rotor with load disturbance	54
4.24	Comparison between current I_a , I_b and I_c	55
4.25	Zoom view during the starting current at load disturbance	55
4.26	Comparison between reference speed, speed estimator and actual speed with load disturbance	56
4.27	Zoom view of speed during load disturbance	56

FIGURE	TITLE	PAGE
4.28	Comparison between actual position and position estimator of rotor with load disturbance	57
4.29	Comparison between current I_a , I_b and I_c with load disturbance	58
4.30	Zoom view during the starting current at load disturbance	58
4.31	Comparison between reference speed, speed estimator and actual speed with load disturbance	59
4.32	Zoom view of speed during load disturbance	59
4.33	Comparison between actual position and position estimator of rotor with load disturbance	60
4.34	Comparison between current I_a , I_b and I_c with load disturbance	61
4.35	Zoom view during the starting current at load disturbance	61



اونيورسيتي تيكنيكل مليسيا ملاك

UNIVERSITI TEKNIKAL MALAYSIA MELAKA

LIST OF ABBREVIATIONS

PMSM	-	Permanent Magnet Synchronous Machine
FOC	-	Field Oriented Control
EMF	-	Electro Motive Force
EVs	-	Electric Vehicles
AC	-	Alternating Current
DC	-	Direct Current
SVPWM	-	Space Vector Pulse Width Modulation
PM	-	Permanent Magnet
T	-	Operation Times
PI	-	Proportional Integral
Kp	-	Proportional Controller
Ki	-	Integral Controller
PWM	-	Pulse Width Modulation
VSI	-	Voltage Source Inverter
THD	-	Total Harmonic Distortion
SVM	-	Space Vector Modulation
R	-	Resistance
L	-	Inductance
IGBT	-	Insulated Gate Bipolar Transistor
DSP	-	Digital Signal Processor
EMI	-	Electro Magnetic Interference

LIST OF SYMBOLS

i_q	-	Current on q -axis
i_d	-	Current on d -axis
V_d	-	Voltage on d -axis
V_q	-	Voltage on q -axis
R_m	-	Resistance Motor
L_{md}	-	Direct-axis Magnetization Inductance
R_s	-	Resistance Stator
Ψ_d	-	Flux on d -axis
Ψ_q	-	Flux on q -axis
V_{dc}	-	Voltage DC source
d, q	-	2-axis rotating frame
α, β	-	2-axis orthogonal
ω	-	Speed of the Motor
e_α	-	α -axis of Back-EMF
e_β	-	β -axis of Back-EMF
i_α	-	Current Alpha
i_β	-	Current Beta
V_α	-	Voltage Alpha
V_β	-	Voltage Beta
L_α	-	Inductance Alpha
L_β	-	Inductance Beta
ϕ_m	-	Maximum Flux
θ	-	Angle
i_{sqref}	-	Reference Stator Phase Currents on q -axis
i_{sdref}	-	Reference Stator Phase Currents on d -axis
t	-	Times
θ_r	-	Angular Rotor Position

LIST OF APPENDICES

APPENDIX	TITLE	PAGE
1	Project Gant Chart	70
2	Configuration of Sensorless Speed Control in Vector Controlled PMSM Drives	71



اونيورسيتي تيكنيكل مليسيا ملاك

UNIVERSITI TEKNIKAL MALAYSIA MELAKA

CHAPTER 1

INTRODUCTION

1.1 Introduction

The permanent magnet synchronous machine (PMSM) has been commonly used in industrial application [2]. This is because a lot of the advantages of PMSM such as high power density and efficiency, high torque to inertia ratio, easy to control and high reliability. Other than that, in higher performance applications of machine drive, the PMSM drive are ready to use in sophisticated requirements such as fast dynamic response, high power factor and wide operating on the speed range [3]. This has opened up new possibilities for large scale application of PMSM drive.

The PMSM drive using field oriented control (FOC) or vector control techniques need an exact position of the rotor and speed estimator for the current and speed control. Other than that, the sensorless have been more popular for the AC motor drive because their system is easier to implement and have a low cost by removing position feedback. In addition, there is no fault occurred when the motor shaft misaligned to the position sensor in the production process [6].

This report presents and discusses a sensorless control algorithm for permanent magnet synchronous motor (PMSM) drives based on the back Electro Motive Force (EMF) to determine the rotor position and speed estimation. Estimation of the back EMF is made by the reference voltages given by the current controller. This research will be conducted by using a SIMULINK/MATLAB software. The result will be discussed at the end of the research.

1.2 Motivation

In the last years, given the increase in oil consumption, such as by cars, there is a fast growing interest to find another source of non-polluting energy. For this in the automotive field, the industry has opted for the use of electric vehicles (EVs). However, the energy storage is the weak point of EVs that delays their progress. For this reason, the motor scheme development needs to build more efficient, lightweight, compact and electric propulsion systems, to maximize driving range per charge [10].

In addition, the control planning developed for variable speed drives working on PMSM are based of the current control on space vector in a rotor frame. This method requires the knowledge of the rotor shaft position for coordinate transformations and information about the speed. The applications of PMSM drive, the rotor position signal is obtained from a mechanical sensor that will reduce the reliability of the system and added the cost of the drives [2]. Therefore, a strong desire arises in the alternative of PMSM sensorless control, where the estimators are employed as transducers software or electronic commutation to provide the feedback data required by the control system.

1.3 Problem Statement

The vector control of a PMSM requires knowledge of the rotor shaft position and information on the speed. These mechanical quantities of a PMSM have usually been measured by shaft mounted motion sensors such as a tachometer, an encoder and resolvers. Based on the previous research by Fabio Genduso, on “Back-EMF Sensorless Control Algorithm for High Dynamics Performances PMSM” discover that the availability of these sensors, there are some of several disadvantages using that methods such as additional system cost, a higher number of connections between the motor and the frequency converter and reduced robustness [13]. Other than that, in an industrial environment using these sensors are easily damaged by mechanical impacts, especially in lower power ranges the motion sensor can be the most expensive component in the entire drive system. For this reason several strategies to detect the speed and position without sensors have been developed for PMSM [3].

1.4 Objective

The main objectives of this project are:

- i. To model and simulate a position and speed estimator based on back-EMF sensorless control for PMSM using SIMULINK/MATLAB software.
- ii. To analyze the performance of sensorless operation related to the back-EMF of the PMSM.

1.5 Project Scope

The project scope is the limitations for each project that have been conducted. The scope of this project are:

- i. Focus on position and speed estimation of PMSM sensorless drives
- ii. Model and simulate using MATLAB/SIMULINK software.
- iii. Analyze the performance of the back-EMF based on measurement phase currents and voltages.
- iv. Design and develop position and speed estimator algorithms.

1.6 Project Outline

This paper is organized as follows; Chapter 2 introduces the basic principle about permanent magnet synchronous machine (PMSM) model, field-oriented control (FOC), space vector pulse width modulation (SVPWM) and back-EMF. Chapter 3 describes about the method that will be used to conduct to do this project until success. Chapter 4 describes about the result and analysis that will come out of this project. Finally, conclusions and recommendation are presented in Chapter 5.

CHAPTER 2

LITERATURE REVIEW

2.1 Theory And Basic Principles

In this chapter it is basically more on the understanding the literature review of a permanent magnet synchronous machine (PMSM) model. This chapter presents the review of PMSM principle when using back-EMF in sensorless control. The reviews are from the recent and past journals, technical papers and reference books which have been studied to understand the related topic area of this project. In addition, this chapter will go through deeply regarding PMSM sensorless control using back-EMF such as its principle, equation and about the testing used in order to know the properties of the PMSM.

2.1.1 Permanent Magnet Synchronous Machine (PMSM)

A PMSM is a motor drive that uses permanent magnets to produce the air gap magnetic field rather than using electromagnets. The power density of PMSM is higher than one of induction motors with the same ratings due to the no stator power dedicated to the magnetic field production. PMSM is designed not only to be more powerful but also with lower mass and lower moment of inertia [1]. Permanent magnet motors, one of the magnetic fields is created by permanent magnets and the other is created by the stator coils. The maximum torque is produced when the magnetic vector of the rotor is at 90° to the magnetic vector of the stator [1].

2.1.1.1 PMSM Drive System

The motor drive consists of four main components, which are the PM motor, inverter, and the position sensor. The components are connected as shown in Figure 2.1.

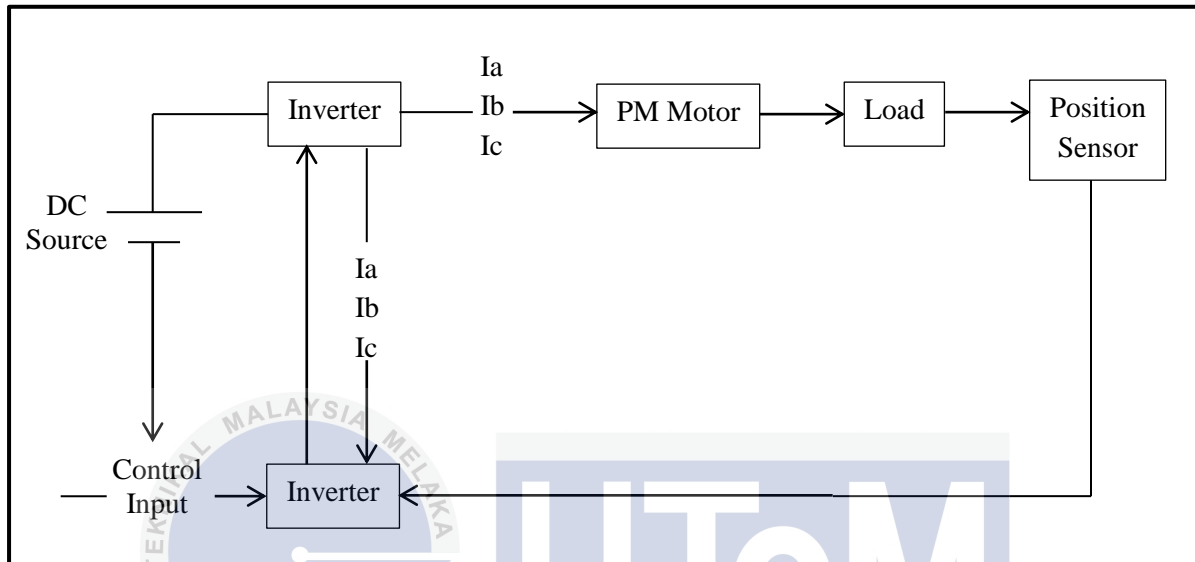


Figure 2.1: Basic block diagram of PMSM

This is a description of the block diagram of PMSM in Figure 2.1.

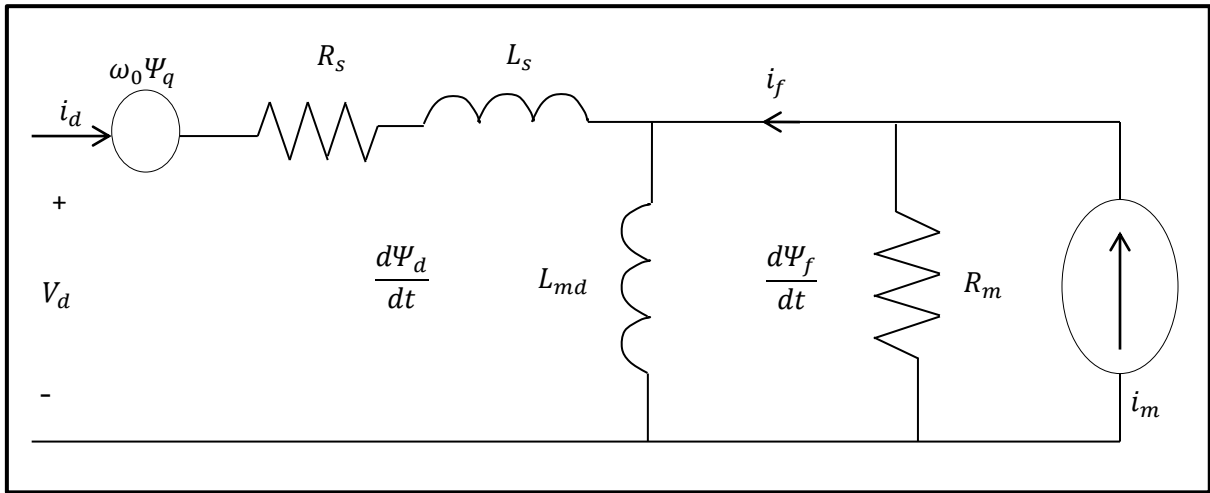
i. Inverter

Convert a DC voltage to AC voltage of variable frequency and magnitudes. It also use for adjustable speed drives and are characterized by a well defined switched voltage wave form in the terminals [9].

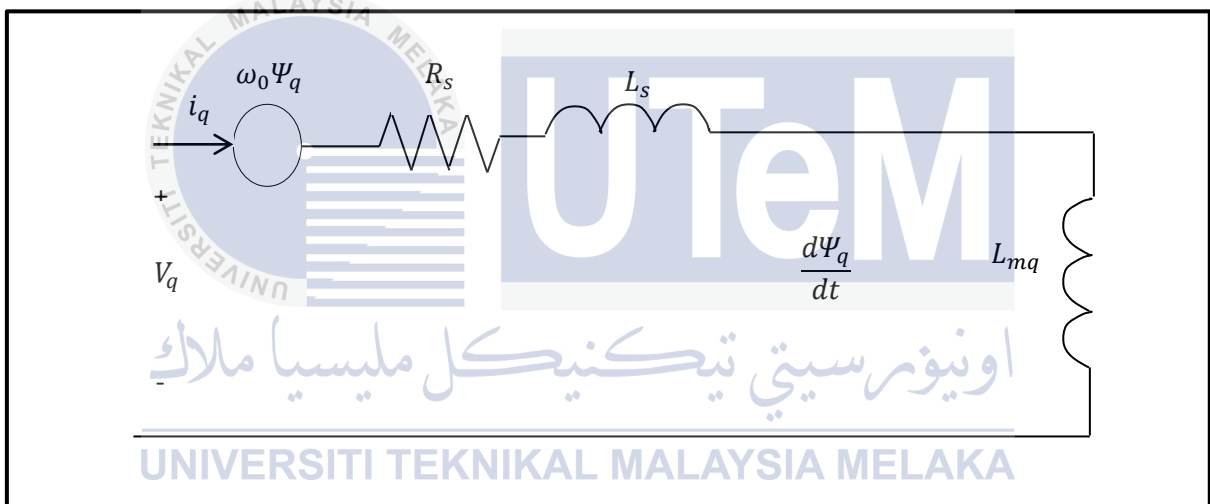
ii. Position sensor

Requires position sensors in the rotor shaft when operated without damper winding and the development of devices for position measurement [9].

2.1.1.2 Modelling Of PMSM



(a)



(b)

Figure 2.2: Equivalent circuit of the PMSM (a) d -axis (b) q -axis

Where i_d and i_q is d -axis and q -axis current. V_d and V_q is d -axis and q -axis input voltage. Constant current source, i_m located at the stator direct axis. Essentially resistance, R_m connected across the direct-axis magnetization inductance, L_{md} shows this effect and no leakage inductance in the field. The permeability of the magnet material is almost unity, so the air gap inductance seen by the stator is the same in direct and quadrature axes and also no saturation will happen inside the machine [4].

From Figure 2.2, the equations for the model PMSM are:

$$\frac{d\Psi_d}{dt} = V_d - R_s i_d - \omega \Psi_q \quad (2.1)$$

$$\frac{d\Psi_f}{dt} = R_m i_m - R_m i_f \quad (2.2)$$

$$\frac{d\Psi_q}{dt} = V_q - R_s i_q + \omega \Psi_d \quad (2.3)$$

2.1.2 Field Oriented Control (FOC)

The Field Orientated Control (FOC) as known as vector control consists of controlling the stator currents represented by a vector. This control is based on the projections which transform a three-phase time and speed dependent system into a two coordinate (d and q coordinates) time invariant system. These projections lead to a structure similar to that of a DC machine control. FOC machines need two constants as input references, which are torque component (aligned with the q coordinate) and flux component (aligned with the d coordinate) [4].

As FOC is simply based on projections the control structure handles instantaneous electrical quantities. This makes the control accurate in every working operation it is in steady state and transient. Beside that, it also independent of the limited bandwidth on mathematical model [4].

2.1.2.1 The Basic Block Diagram Of The FOC

The diagram summarizes the basic scheme of torque control with FOC.

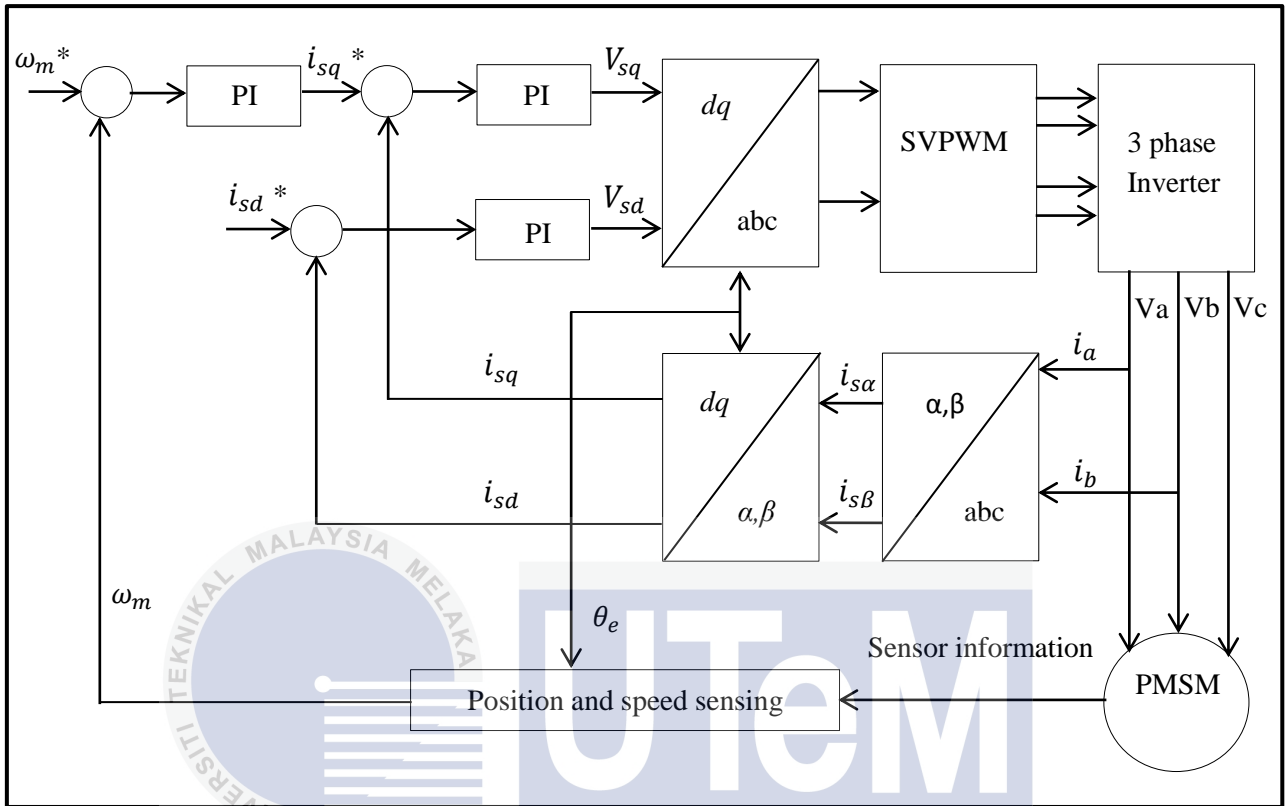


Figure 2.3: Basic scheme of FOC for AC motor

From the Figure 2.3, i_a and i_b are measured with a current sensor. The clarke transformation are applied to it to determine the stator current projection in a two coordinates nonrotating frame. The park coordinate transformation is then applied in order to obtain this projection in the (d, q) rotating frame. The (d, q) projections of the stator phase currents are then compared to their reference values i_{sqref} and i_{sdref} is set to zero and corrected by PI current controllers. The outputs of the current controllers are passed through the inverse park transformation and a new stator voltage vector is impressed to the motor using the space vector modulation technique. In order to control the mechanical speed of the motor (ω), an outer loop is driving the reference current, i_{sqref} [6].

2.1.3 Proportional Integral (PI) Controller

PI Controller (proportional integral controller) is a feedback controller which drives the plant to be controlled with a weighted sum of the error (difference between the output and desired set point) and the integral of that value [9]. The motion control system often utilizes a proportional integral (PI) controller. Which is the P controller in the position loop and PI Controller in the speed and torque loop are often adequate. PI controller consists K_p and K_i where K_p is proportional-controller gain and K_i is the integral-controller gain [10]. It's implemented in this transfer function to obtain zero steady-state error and good dynamic responses such as fast transient responses with minimum overshoot and make the system less sensitive to disturbances and changes in the system parameters.

2.1.4 Space Vector

The three-phase voltages, currents and fluxes of AC motors can be analyzed in terms of complex space vectors. From the currents, the space vector can be defined, if assuming that i_a, i_b, i_c are the instantaneous currents in the stator phases, then the complex stator current vector i_s will be defined by:

$$i_s = i_a + \alpha i_b + \alpha^2 i_c \quad (2.4)$$

Where;

$$\alpha = e^{j\frac{2\pi}{3}} \quad (2.5)$$

$$\alpha^2 = e^{j\frac{4\pi}{3}} \quad (2.6)$$

From Equation 2.5 and 2.6 its represent the spatial operators. The following diagram shows the stator current complex space vector:

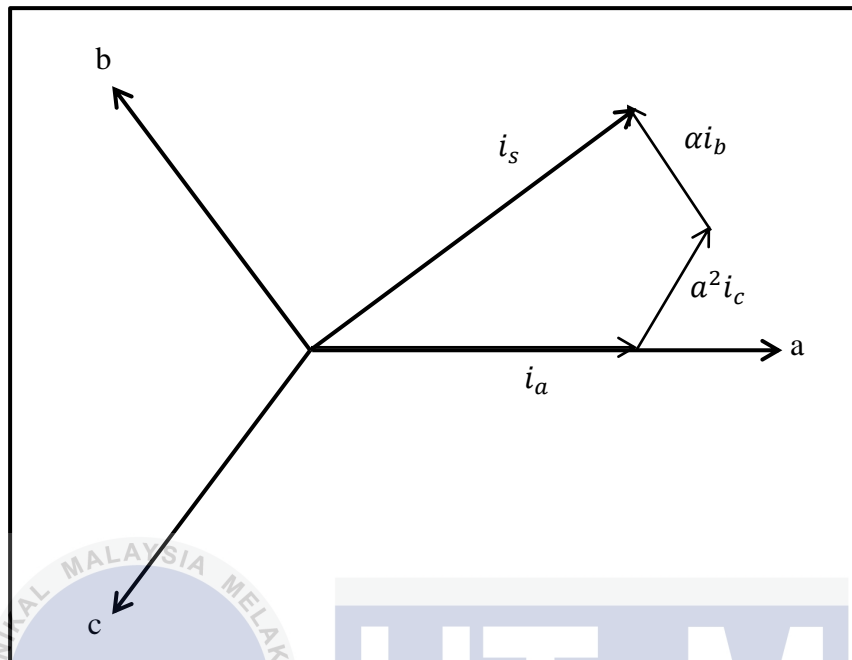


Figure 2.4: Stator current space vector and its component in (a, b, c)

Where (a, b, c) are the three-phase system axes. This current space vector shown the three-phase sinusoidal system. The transformation from the three-phase 120° reference frame to two-axis orthogonal reference frame is known as clarke transforms. While, the transformation from two-axis orthogonal reference frame to the two-axis rotating reference frame is known as park transform [6].

i. Clarke transformation

This transformation converts balanced three-phase quantities into balanced two-phase quadrature quantities. The three-phase quantities are translated from the three-phase reference frame to the two-axis orthogonal stationary reference frame using clarke transformation. The measured motor currents are first translated from the three-phase reference frame to the two-axis orthogonal reference frame.

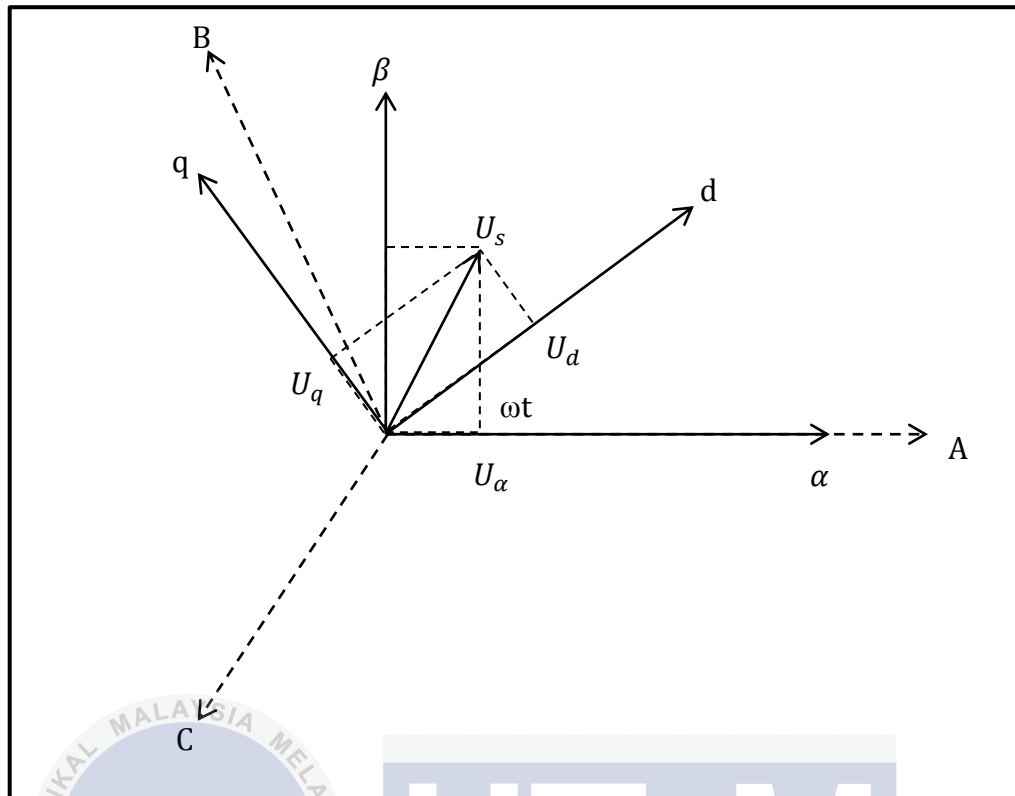


Figure 2.5: Clarke transformation using reference frame

The transform is expressed by the following equations [6] :

$$\begin{bmatrix} u_\alpha \\ u_\beta \\ u_0 \end{bmatrix} = \begin{bmatrix} \frac{2}{3} & \frac{1}{3} & \frac{1}{3} \\ 0 & \frac{1}{\sqrt{3}} & \frac{-1}{\sqrt{3}} \\ \frac{1}{3} & \frac{1}{3} & \frac{1}{3} \end{bmatrix} \begin{bmatrix} u_a \\ u_b \\ u_c \end{bmatrix}$$

(2.7)

$$i_{s\alpha} = i_a$$

(2.8)

$$i_{s\beta} = (i_a + 2i_b)/\sqrt{3}$$

(2.9)

Where;

$$i_a + i_b + i_c = 0$$

(2.10)

ii. Park transformation

The two-axis orthogonal stationary reference frame quantities are transformed into rotating reference frame quantities using park transformation. The two-axis orthogonal system (α, β) in the two axis rotating reference frame (d, q) . If we consider the d -axis aligned with the rotor flux. In the Figure 2.6 shows for the current vector and the relationship of two reference frame [6].

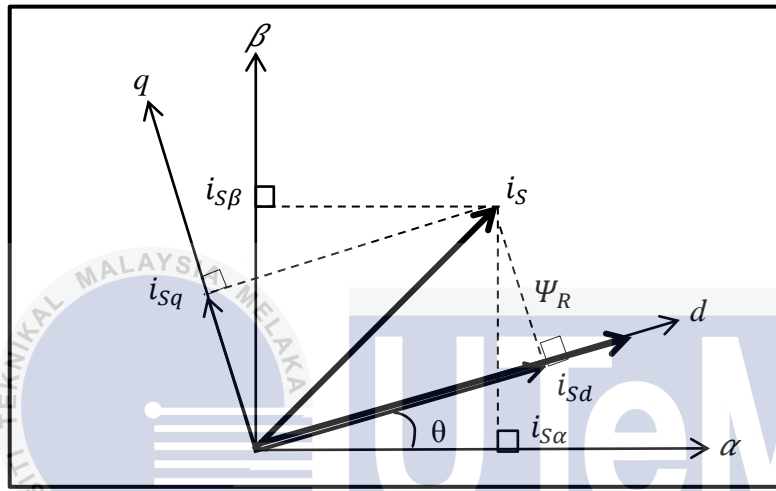


Figure 2.6: Stator current space vector and its component in (a, b) and in the d, q rotating reference frame

The transform is expressed by the following equations:

$$u_\alpha + ju_\beta = (u_d + ju_q) e^{-j\omega t} \quad (2.11)$$

$$\begin{bmatrix} u_\alpha \\ u_\beta \\ u_0 \end{bmatrix} = \begin{bmatrix} \cos(\omega t) & -\sin(\omega t) & 0 \\ \sin(\omega t) & \cos(\omega t) & 0 \\ 0 & 0 & 1 \end{bmatrix} \cdot \begin{bmatrix} u_d \\ u_q \\ u_0 \end{bmatrix} \quad (2.12)$$

$$i_{sd} = i_{s\alpha} \cos\theta + i_{s\beta} \sin\theta \quad (2.13)$$

$$i_{sq} = -i_{s\alpha} \sin\theta + i_{s\beta} \cos\theta \quad (2.14)$$

iii. Inverse Clarke transformation

The transformation from two-axis orthogonal stationary reference frame to the three-phase stator stationary reference frame is accomplished using the inverse clarke transformation [5].

The inverse clarke transformation is expressed by the following equations:

$$\begin{bmatrix} u_a \\ u_b \\ u_c \end{bmatrix} = \begin{bmatrix} 1 & 0 & 1 \\ -\frac{1}{2} & \frac{\sqrt{3}}{2} & 1 \\ -\frac{1}{2} & -\frac{\sqrt{3}}{2} & 1 \end{bmatrix} \begin{bmatrix} u_d \\ u_q \\ u_0 \end{bmatrix} \quad (2.15)$$

$$V_{saref} = V_{saref} \quad (2.16)$$

$$V_{sbref} = [-V_{saref} + \sqrt{3} \cdot V_{sqref}] / 2 \quad (2.17)$$

$$V_{scref} = [-V_{saref} - \sqrt{3} \cdot V_{sqref}] / 2 \quad (2.18)$$

iv. Inverse Park transformation

The outputs of the PI controllers provide the voltage components in the rotating reference frame. Thus an inverse of the previous process has to be applied to get the reference voltage waveforms in a stationary reference frame. At first, the quantities in a rotating reference frame are transformed to two-axis orthogonal stationary reference frame using inverse park transformation [4]. The inverse park transformation is expressed by the following equations:

$$\begin{bmatrix} u_a \\ u_b \\ u_c \end{bmatrix} = \begin{bmatrix} \cos(\omega t) & -\sin(\omega t) & 1 \\ \cos\left(\omega t - \frac{2\pi}{3}\right) & -\sin\left(\omega t - \frac{2\pi}{3}\right) & 1 \\ \cos\left(\omega t + \frac{2\pi}{3}\right) & -\sin\left(\omega t - \frac{2\pi}{3}\right) & 1 \end{bmatrix} \begin{bmatrix} u_d \\ u_q \\ u_0 \end{bmatrix} \quad (2.19)$$

$$V_{saref} = V_{sdref} \cos\theta - V_{sqref} \sin\theta \quad (2.20)$$

$$V_{sbref} = V_{sdref} \sin\theta + V_{sqref} \cos\theta \quad (2.21)$$

2.1.5 Space Vector Pulse Width Modulation (SVPWM)

Space vector modulation (SVM) is an algorithm for the control of pulse width modulation (PWM). It is used for the creation of alternating current (AC) waveforms most commonly to drive three phase AC powered motors at varying speeds from DC voltage [14]. There are various variations of SVM that result in different quality and computational requirements. One active area of development is in the reduction of total harmonic distortion (THD) created by the rapid switching inherent to these algorithms.

Variable voltage and frequency supply to AC drives is invariably obtained from a three-phase voltage source inverter (VSI). A number of pulse width modulation (PWM) scheme is used to obtain variable voltage and frequency supply. The most widely used PWM schemes for three-phase VSI are carrier-based sinusoidal PWM and SVPWM. A three-leg voltage source inverter (VSI) providing two-phase outputs is increasingly interesting for two-phase drive applications due to good DC voltage utilization, reduced THD of currents, and availability of three-leg modules [15]. Because of the constraint that the input lines must never be shorted and the output current must always be continuous a VSI can assume only eight distinct topologies. These topologies are shown in Figure 2.9. Six out of these eight topologies produce a non-zero output voltage and are known as non-zero switching states and the remaining two topologies produce zero output voltage and are known as zero switching states.

A mathematical model of three-phase is presented here based on space vector representation. The power circuit topology of a three-phase VSI is shown in Figure 2.7. Each switch in the inverter leg is composed of two back-to-back connected semiconductor devices. One of these two is a controllable device and another one is a diode for protection. The voltage waveform is shown in Figure 2.8 for 180° conduction mode. It is observed one inverter leg's state changes after an interval of 60° and their state remains constant for 60° interval. Thus, it follows that the leg voltages will have six distinct and discrete values in one cycle, which is equivalent to 360° .

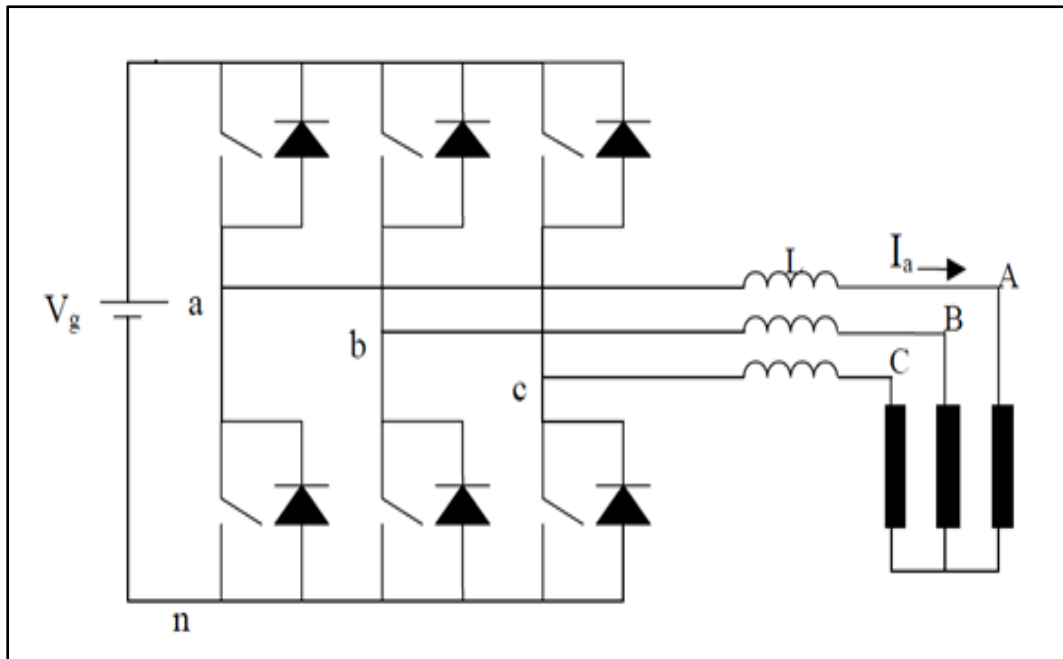


Figure 2.7: Topology of a three-leg voltage source inverter

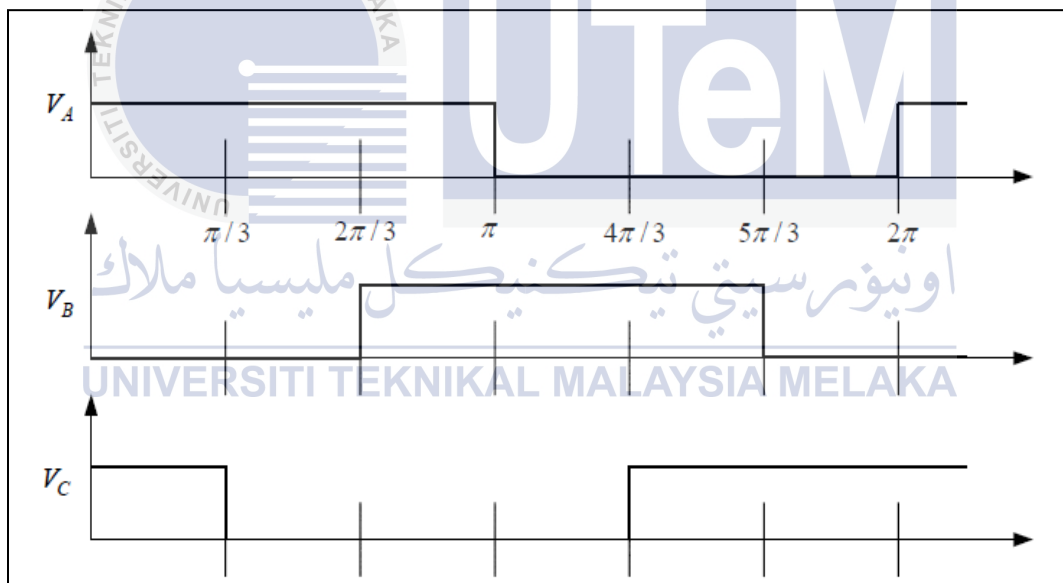


Figure 2.8: Voltage waveforms of a three-phase VSI

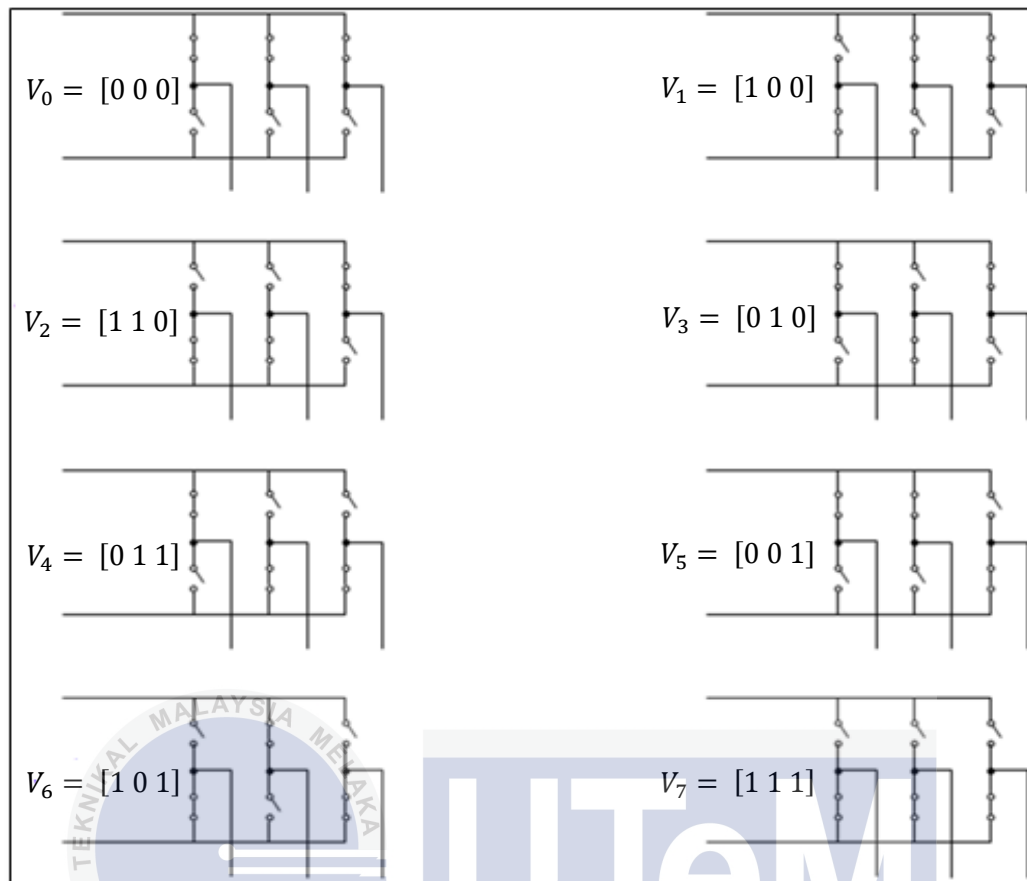


Figure 2.9: Eight switching state topologies of a voltage source inverter

SVPWM aims to generate a voltage vector that is close to the reference circle through the various switching modes of the inverter. For the ON-OFF state of the three-phase inverter circuit, each phase can be considered as a switch (S). $S_A(t)$, $S_B(t)$ and $S_C(t)$ is used as the switching functions for the three phases, respectively. The space vector of output voltage of the inverter can be expressed as:

$$V_{an} = \frac{V_{dc}}{3} (2S_a - S_b - S_c) \quad (2.22)$$

$$V_{bn} = \frac{V_{dc}}{3} (2S_b - S_c - S_a) \quad (2.23)$$

$$V_{cn} = \frac{V_{dc}}{3} (2S_c - S_a - S_b) \quad (2.24)$$

Where V_{dc} is the DC bus voltage of inverter and $\alpha = e^{j120}$. The expression of the state of the upper-arm with “1” and the off state with “0”, the ON-OFF states of three phases have eight combinations, correspondingly forming eight voltage space vectors, as

shown in Figure 2.10. T refers to the operation times of two adjacent non-zero voltage space vectors in the same zone. Both $V_0(000)$ and $V_7(111)$ are called the zero voltage space vector and the other six vectors are called the effective vector with a magnitude of $2V_{dc}/3$. For the example, when the output voltage vector V is within zone one, it is composed of V_4, V_6, V_0 and V_7 . It can be obtained by $V_{out} = T_4V_4/T + T_6V_6/T$. The eight ON-OFF states of inverter are listed in Table 2.1.

Table 2.1: Eight ON-OFF states of the inverter

Inverter state	$S_A S_B S_C$	$S_{\bar{A}} S_{\bar{B}} S_{\bar{C}}$	$\frac{V_A}{V_{dc}}$	$\frac{V_B}{V_{dc}}$	$\frac{V_C}{V_{dc}}$
0	000	111	0	0	0
1	001	110	-1/3	-1/3	2/3
2	010	101	-1/3	2/3	-1/3
3	011	100	-2/3	1/3	1/3
4	100	011	2/3	-1/3	-1/3
5	101	010	1/3	-2/3	1/3
6	110	001	1/3	1/3	-2/3
7	111	000	0	0	0

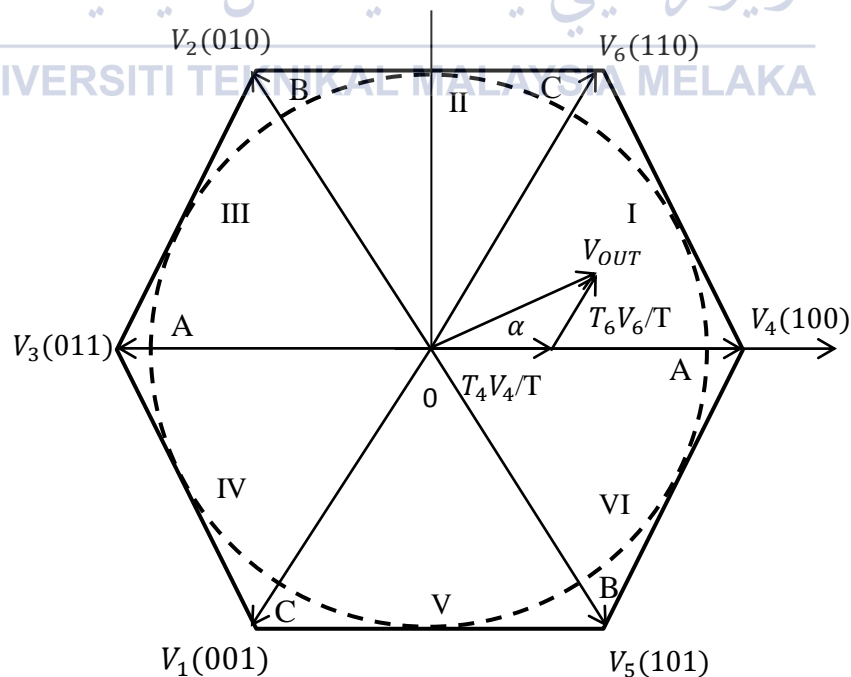


Figure 2.10: Diagram of voltage space vector

Where $e_{\alpha\beta}, \Psi_{\alpha\beta}, V_{\alpha\beta}$ and $i_{\alpha\beta}$ are respectively the back-EMF, flux linkages, terminal voltages and phase currents in α - β frame, and R the winding resistance.

The flux linkages are generated in term of position as:

$$\begin{aligned}\Psi_{\alpha} &= L_{\alpha}i_{\alpha} + \phi_m \cos\theta \\ \Psi_{\beta} &= L_{\beta}i_{\beta} + \phi_m \sin\theta\end{aligned}\quad (2.27)$$

Where θ, ϕ_m and $L_{\alpha,\beta}$ are respectively the actual rotor angle, maximum flux linkage of the permanent magnet and inductances in α - β frame. Equation 2.25, 2.26 and 2.27 is an electrical and magnetic equations are the basis for the position and speed extraction from the voltage and current measurement.

The back-EMF which is calculated based of the voltage and current measurements, is supposed to be accurate and then contains the actual position. So the equations is [11]:

$$\begin{aligned}e_{\alpha} &= \frac{d\Psi_{\alpha}}{dt} = L \frac{di_{\alpha}}{dt} - \omega\phi_m \sin\theta \\ e_{\beta} &= \frac{d\Psi_{\beta}}{dt} = L \frac{di_{\beta}}{dt} - \omega\phi_m \cos\theta\end{aligned}\quad (2.28)$$

Given an estimated angle, Equation 2.27 is used to estimate the flux vector components:

$$\begin{aligned}\Psi_{\alpha} &= Li_{\alpha} + \phi_m \cos\theta \\ \Psi_{\beta} &= Li_{\beta} + \phi_m \sin\theta\end{aligned}\quad (2.29)$$

2.1.7 Back-EMF Using Sensorless Control

The back-EMF is an inductive components like motor winding resist sudden changes in current. Because of that the magnetic field caused by the current needs time to build up or decrease. That means, when current is flowing and this is suddenly cut off, the winding will try to maintain that current and becomes a power source generating a voltage.

It gets its power from the built up of magnetic field. Since the winding has become a power source, the voltage is reversed for the same current flow direction [10]. That also explains how the voltage on a coil can become higher than the power supply.

Nowadays, the back-EMF based sensorless algorithm has been already combined with the vector control method in many industrial applications [7]. The performance of the back-EMF based sensorless vector control is mainly determined by the sensorless algorithms with relate to the position and speed estimation. The back-EMF based methods are to be operated in medium to high speed range. The back-EMF based sensorless algorithm suffers from the small amplitude of back-EMF signals at low speed. Therefore, the signal uncertainty may cause system unstable or even operation failure [7].

2.1.7.1 Back-EMF Based Sensorless Algorithm

The subchapters will describes a voltage vector equation in Equation 2.30 and a phasor diagram in Figure 2.12. The conventional back-EMF sensorless algorithm is based on the back-EMF orientation in the stator.

The equation is: اونيورسيتي تيكنيكل مليسا

$$U = RI + j\omega LI + E \quad (2.30)$$

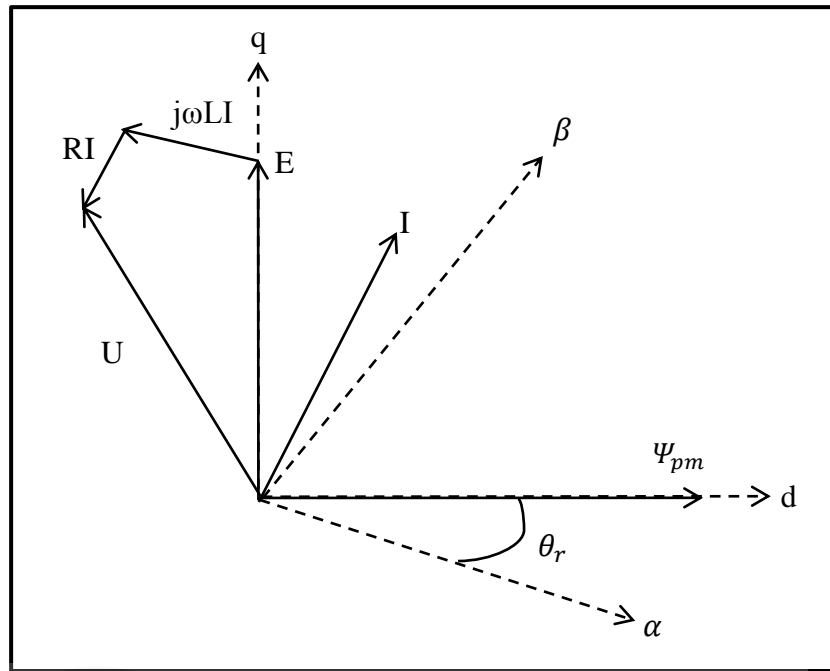


Figure 2.12: Phasor diagram of PMSM

Where Ψ , u and i are the stator flux linkage, phase voltage and phase current. The α and β stands for their corresponding $\alpha\beta$ components. R_s is the stator phase resistance, L_s is the average dq inductance, which can be defined as:

$$L_s = (L_d + L_q)/2 \quad (2.31)$$

From Equation 2.31, it is shown the permanent magnetic flux. θ_r is the rotor angular position in electrical radians [10].

In order to operate the back-EMF sensorless algorithm, the parameters need to be known are the stator resistance and the stator inductance. The variables need to be measured are just stator phase currents. Since the stator voltages are obtained by PWM signal reconstruction from DC voltage and can be adjusted automatically by current loops [8], then no need for voltage measurement.

2.2 Comparison with other method of sensorless

PMSM drive research has been concentrated on the elimination of the mechanical sensors at the motor shaft without deteriorating the dynamic performances of the drive. Many advantages of sensorless AC drives such as reduced hardware complexity, low cost, reduced size, cable elimination, increased noise immunity, increased reliability and decreased maintenance. That has been a review of difference speed and rotor position estimation schemes of PMSM drives has been introduced. Besides that, that have many the type of sensorless method that has been review such as back-EMF, magnetic saliency or saturation effect, instantaneous power and other more.

Table 2.2 shown comparison between other method of sensorless that has been use for PMSM.

Table 2.2: Comparison other method

Method	Problems
1. Instantaneous power	<ul style="list-style-type: none"> • Variable switching frequency. • Solution requires a fast microprocessor and analogue/digital converters.
2. Magnetic saliency /saturation effect	<ul style="list-style-type: none"> • Attractive at low speed region but the noise by diagnose signal degrades the electromagnetic interference specification. • The extra circuit for injecting a high frequency signal is necessary.

2.3 Previous Related Works

Permanent magnet synchronous machine (PMSM) drive is a main topic of this project. A some research was carried out referring to a journal of previous research as a benchmark of this project. There are three different journals had been studying about the

modelling and simulation of the drives and controllers that used to achieve the objectives in this project.

A PMSM drive is a power converter and a controller is the major components of an PMSM drive system. Some of the related to these components are electric machine design, electric machine modeling, sensing and measurement techniques, signal processing, power electronics design and electric machine control. It will be the main issue that focus on the related of the PMSM control [8]. A PMSM sensorless control using back-EMF based on position and speed estimation method can be used to control the machine in certain conditions [9]. This chapter review the previous related work of the sensorless control of the machines drives and outline the major problems in its design and implementation.

The first paper is authored by Youness Alite Driss and Driss Yousfi the titled “PMSM sensorless control using back-EMF based position and speed estimation method” [11]. This paper is about a position and speed estimation method based on the measurement of phase currents and voltages of the PMSM drive model. The purpose is to elaborate a precise estimator in accordance with some specifications, especially the ability to cancel position error. In addition, the sensorless control method is used to provide satisfactory efficiency. The control schemes developed for variable speed drives working on synchronous machines are based on control of the current space vector in a rotor frame. This strategy requires knowledge of the rotor shaft position for coordinate transformations and the necessary information on speed. The back-EMF method of position and speed estimation are used in this research. The back-EMF method operated in the medium speed range to high speed range, because the back-EMF based on sensorless algorithm method have the small amplitude of back-EMF signals in low speed range. Motor speed is calculated from position using a backward difference approximation. Position and speed are measured to used only for comparison with the estimates. The objective of this paper is to develop and investigate the mechanical quantities using back-EMF method. The experimental results prove the successful sensorless control with the proposed position and speed estimation method. As a result of applying this method the performance of the wide speed range of this system is very well and the position error is measured to insignificant.

The second paper is authored by Zihui Wang, Qinfen Lu, Yunyue Ye, Kaiyuan Lu and Youtong Fang under the titled “investigation of PMSM back-EMF using sensorless control with parameter variations and measurement errors” [12]. This paper presents performance of sensorless control of PMSM. It needs an accurate and stable estimation of rotor position and speed estimation. From this research, that has several parameter uncertainties and variable measurement errors due to estimation error, such as resistance and inductance variations due to temperature and magnetic flux, current and voltage errors due to measurement uncertainties, and signal delay due to mechanical parts. This paper shows the principles for the performance of the back-EMF based sensorless algorithm. The performance of the back-EMF based sensorless vector control is determined by the sensorless algorithms for the rotor position and speed estimation. Dose this project, vector control method suitable to use for PMSM drive. It gives mathematical analysis and experimental results to support the principles and measure the effects. From the analysis, the back-EMF based sensorless estimation method works well from medium speed range to high speed range. However, if have unexpected errors from parameters and variables the estimated rotor position may vary from its true value and make the system unstable. From this case study, the aspect of the estimated position error is resistance variation caused by thermal effects, inductance variation due to current sensor uncertainties, voltage loss due to insulated-gate bipolar transistor (IGBT) dead-time effect and pulse-width modulation (PWM) signal delay due to digital signal processor (DSP). After making a comparison from all the estimated errors, PWM signal delay is the most higher error which it can be accurately compensated. In addition, to get higher estimation accuracy is to review d - q inductances according flux saturation in the stator.

The third paper is reviewed authored by Fabio Genduso, Cosimo Rando and Giuseppe Ricco Galluzo was titled “ back-EMF sensorless control algorithm for high dynamic performances PMSM” [13]. This paper reviews the control algorithm which based on the estimation of rotor speed and angular position starting from the back-EMF for space vector estimation without voltage sensors by using the reference voltages given by the current controllers. This choice obviously introduces some errors that must be clear by a compensating function. The rotor position and speed estimation of an electrical machine can be obtained by several of specific sensors, but it can give some disadvantages, such as the cost of the sensors and it’s an element of weakness in the motor drive. The proposed of estimation algorithm are the position estimation equation and the

process of compensation of the inverter phase lag that also suggests the final mathematical form of the estimation. The mathematical structure of the estimation guarantees a high degree of robustness for parameters changers. The sensorless control technique is the determination of the back-EMF space vector without voltage measurements by using the reference voltages from the actual voltages. Then, the system will reduce cost factor. As a result, the back-EMF method of space vector is used and have some advantages to any other system using flux estimation because of the integrator elimination avoiding the problem of integration drift that required some suitable devices or sub-systems for its compensation. Then, the control system will be less susceptible on the electro-magnetic interference (EMI) external sources. The proposed system is more reliable and cheaper than other a complicated system without loss of performance on the other system. The proposed algorithm control may be considered a good alternative in terms of cost factors and more accurately without lack of performance for motor drive.

2.3.1 Summary Of The Review

From the three journals that have been reviewed, the methods of all the journals have similar, which is a back-EMF sensorless control for PMSM drives but the proposed of each the journals are quite different. The first journals shown the back-EMF method control to elaborate the accuracy of estimator with ability to cancel a position error for a PMSM drive with propose to get the some advantages, such as reduced complex hardware, low cost and reduces size. The second journals shown the all aspects of estimated position errors when use the back-EMF sensorless control of PMSM drive caused by parameter and variable changes of PMSM vector control. The last journal that has been reviewed proven the back-EMF sensorless control algorithm method can make a system of PMSM drive be more efficient and low cost without reducing a performance.

From this reviewed, the first journal is the best reference for this project. The journals have been reviewed detail on PMSM drive and the elimination of mechanical sensors without reducing the performances of that drive. The sensorless control has many advantages such as simple hardware, low cost and reduced size. For the modeling of PMSM, it was proposed a simple equation to construct a permanent magnet drive focuses. Thus, the measured back-EMF of the machine is used to derive an estimation of the rotor

position and speed for sensorless vector control. The sensorless of PMSM drive is demonstrated to operate in a satisfactory manner. The speedy response is very well and the positional error is measured to be insignificant. Comparison of the result with previous research also can be done in order to evaluate the performance of the proposed method.

Table 2.3 shows the summary of the previous related work that have been studied to ease the understanding of simulation process.

Table 2.3: Summary of the previous related work

Paper	Title	Description
1st	PMSM Sensorless Control Using Back-EMF Based Position and Speed Estimation Method.	The sensorless control has many advantages such as reduced hardware complexity, low cost and reduced size.
2nd	Investigation of PMSM Back-EMF Using Sensorless Control With Parameter Variations and Measurement Errors.	The error caused by PWM signal delay is the most dominant one compared to other aspects, which can be accurately compensated.
3rd	Back-EMF Sensorless Control Algorithm for High Dynamic Performances PMSM.	The algorithm may be a very good alternative in terms of economy and precision without lack of performances and exhibits an increase in reliability.

CHAPTER 3

METHODOLOGY

3.1 Introduction

This chapter covers the detail explanation of methodology that is being used to make this project complete and working well. A lot of methodologies or findings from this field mainly generated into journal for others to take advantage and improve as upcoming studies. Every selection and action that has been done while implementing the project will be explained in phase. This part must be done to make sure the project that consists of software development will be developed systematically, smoothly and successfully. The method is used to achieve the objective of the project that will accomplish a perfect result.

3.2 Overall Process Flow of Project

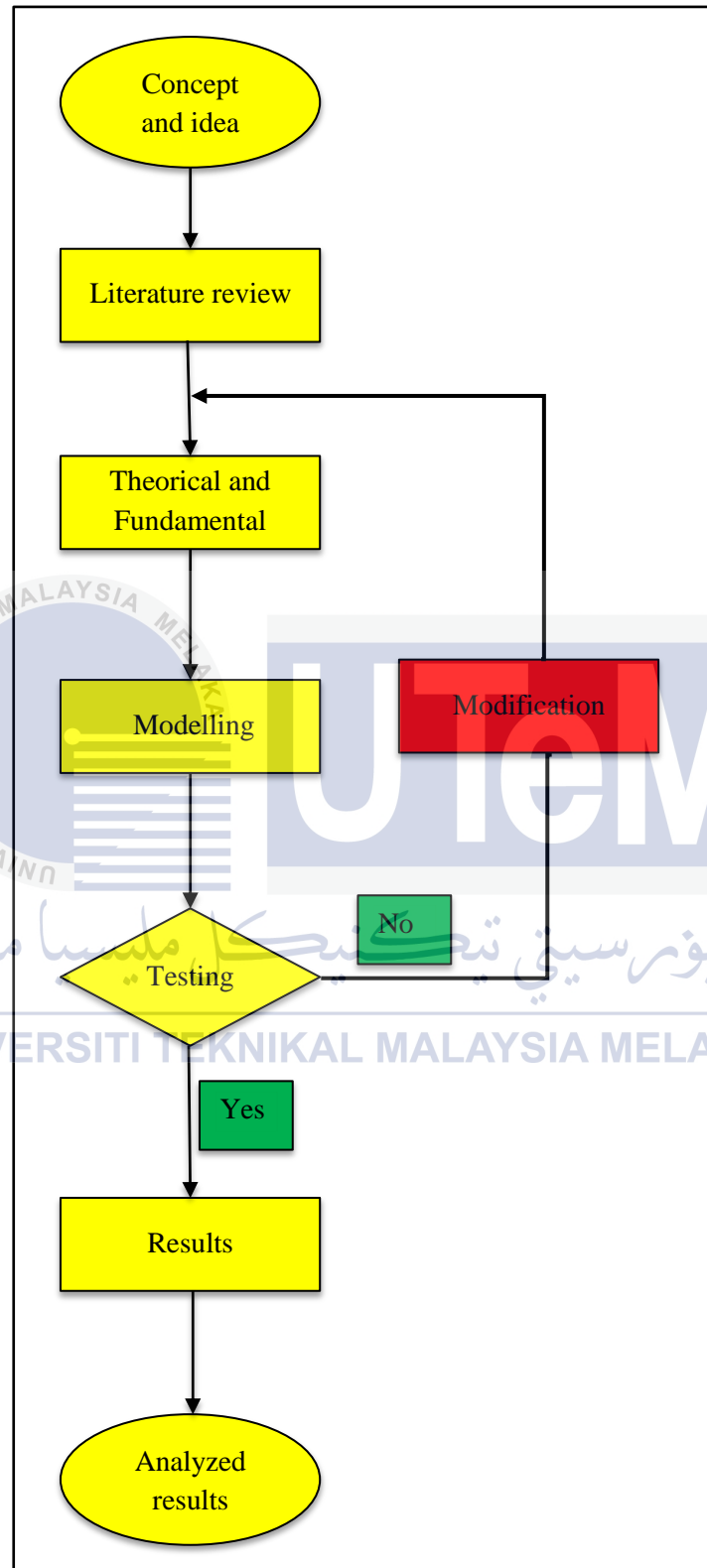


Figure 3.1: Overall project process

3.2.1 Description Of Flow Chart

The flowchart in Figure 3.1 shows the project methodology for this project which consist of concept and idea, literature review, theoretical and fundamental, simulink, testing, modification, result and analyzed results. The flowchart in Figure 3.1 illustrates the flow of modelling of PMSM drive for position tracking and speed estimator based on back-EMF sensorless control using simulation software.

Initially, the research for this project starts with a concept and idea to plan the steps and resources that will be used in this project to be conducted smoothly. At this point, the idea and concept of the project must be understood very well to facilitate progress of the project.

The next step is literature research of the project as well as the basic overall idea for clearer and better understanding. These methodologies consist the literature review of the related research on the journals, articles, internet, books and so on to be analyzed in a proper way. After that, the basic knowledge of the title's project needs to understand very well. This part is necessary to ensure that this project will be completed on time given.

The next flow is the theoretical and fundamental knowledge that need to be performed at this point. Some of the theoretical that had been studied by understanding the basic principle of motor drive can help to conduct this project smoothly because the main purpose of this project is to simulate the whole PMSM drives. There are some types of motor drives had been identified after doing some research such as permanent magnet synchronous motor (PMSM) that will be covered in this research. Then, study the theoretical about PMSM drive model to get some idea to conduct this project in well. The next step is the determination of the appropriate controller to control the parameters of the motor drive which is voltage and current control is used in this project. In this project, sensorless control approach using back-EMF is used. In order to use that approach, the fundamental knowledge that will help the derivation of back-EMF sensorless algorithm, vector control equation and machine drive equation need to be covered to conduct this project.

In the next flow, after learned and familiarized with the SIMULINK/MATLAB software that had to use in this project, simulation process on the PMSM drive by using back-EMF sensorless control is performed. By using this software, it can provide the data required for this case study. Then, a simulation on the PMSM drive by using back-EMF sensorless control method is performed for better understanding by using SIMULIK/MATLAB software.

The following point is the testing point, whereby to ensure that the project fulfill all of the specifications and achieve the objective. The test specification which is the simulation test. This point was designed to ensure that the all of the simulation program work well to get the desired result. If the result of the testing point is not fulfill, the simulation design must be modified. At this point, research on problems that occur in the simulation should be done. After that, make a testing again with the modified of simulation to get the desired results.

After finding out all the results from the simulation process compare the result to analyze the performance of PMSM drive using the simulation process. The data of speed and rotor position are collected from this simulation process. After that, synthesizing all the collected data will be performed. The data will compared between result of estimator and actual result. It will make this research become easier to conduct. For the next, analyzed all the collected data process. This analysis focuses on rotor position error and speed estimation of PMSM design model for sensorless observer. The result of simulation will be shown in next chapter. Lastly, the conclusion of the process can be conclude depend on the result that produced from this simulation process.

3.3 Project Phase

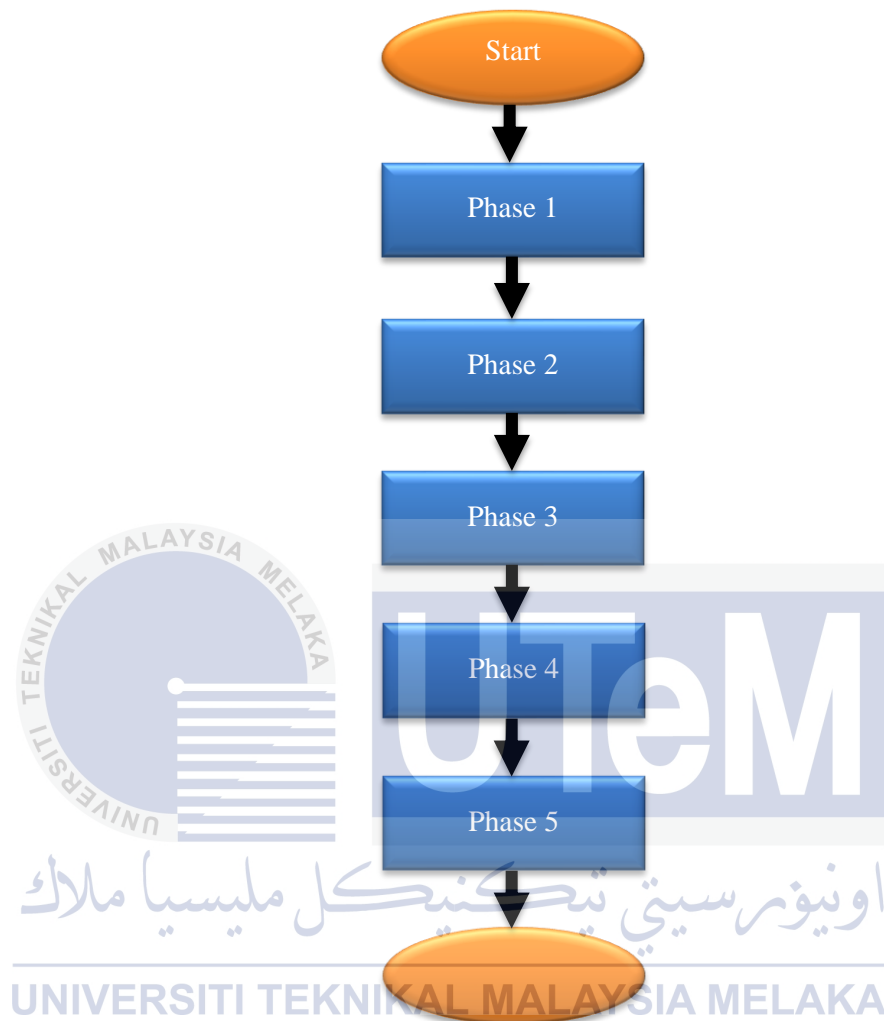


Figure 3.2: Flow of phase project

First phase:

At the beginning of the project, the tasks that have been carried out is about planning the execution of the project, discussion with the supervisor about the project scope and expectation on the project, and writing the proposal for the project.

Second phase:

The literature review is about finding and collecting as much as possible the information and notes to guide the project, which is positioned and speed estimator based on back-EMF for sensorless drivers of permanent magnet synchronous motor (PMSM). There is some mathematical knowledge that needs to understand very well. For understanding the mathematical knowledge it will help to ease of use the estimator equation of PMSM drive for this simulation project

The derivation of back-EMF for sensorless PMSM based on principle of simulation work can be conducted. The back-EMF algorithm that was applied to the feedback sensor or estimator of the drive systems.

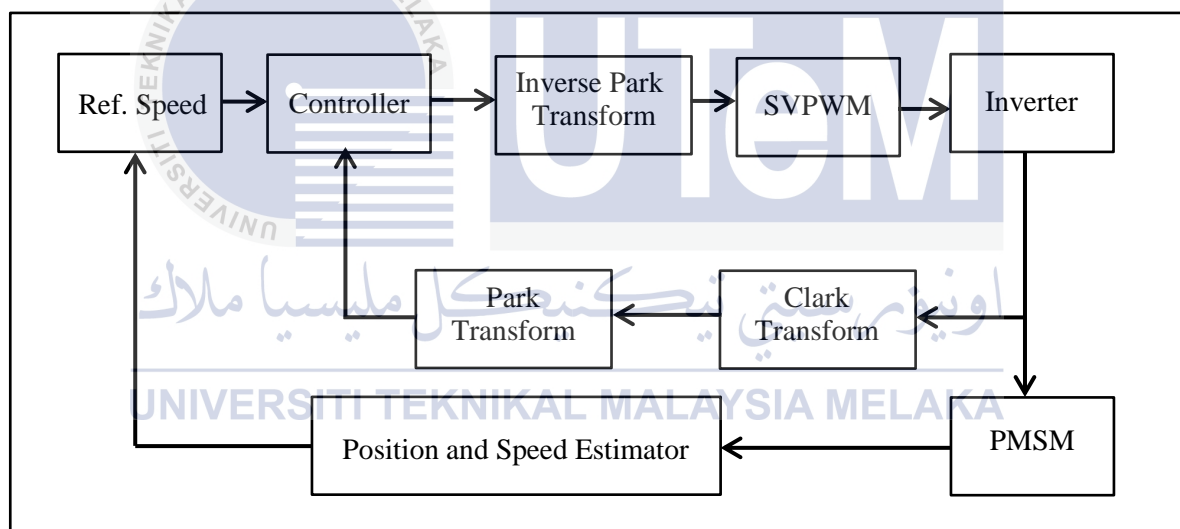


Figure 3.3: Block diagram of the basic motor with estimator

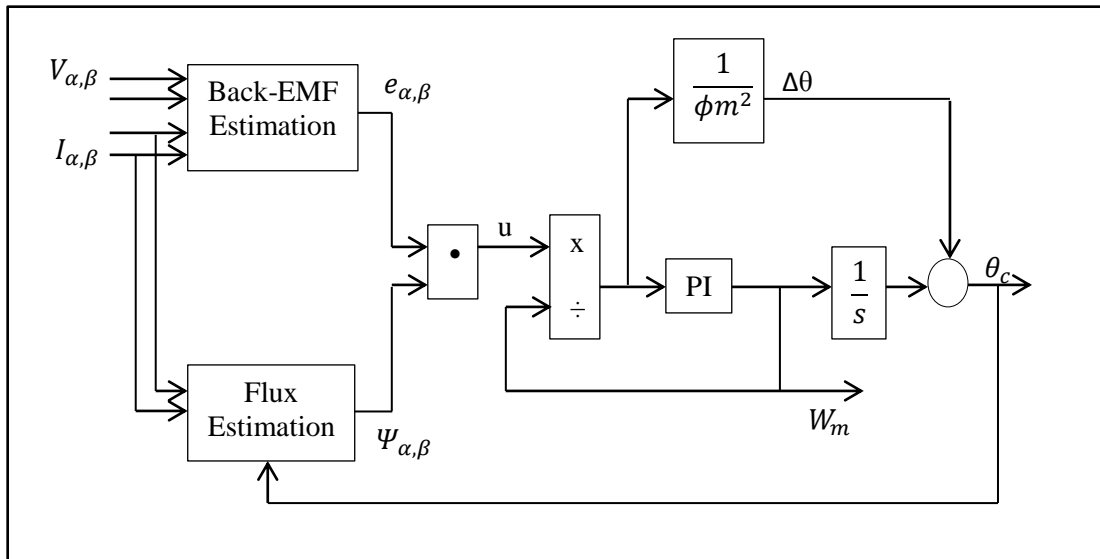


Figure 3.4: Block diagram of the position and speed estimation method

From the Figure 3.4, the equations for modelling estimator are:

$$\begin{aligned} e_{\alpha} &= V_{\alpha} - Ri_{\alpha} \\ e_{\beta} &= V_{\beta} - Ri_{\beta} \end{aligned} \quad (3.1)$$

$$\begin{aligned} \Psi_{\alpha} &= Li_{\alpha} + \phi_m \cos\theta \\ \Psi_{\beta} &= Li_{\beta} + \phi_m \sin\theta \end{aligned} \quad (3.2)$$

Third phase:

At this phase, a simulation on the PMSM drive by using sensorless back-EMF control method is performed for better understanding by using SIMULINK/MATLAB software. The MathWorks library that used to create the blocks in the simulation process. To create the blocks in this process is based on mathematical algorithms that have been studied.

Among of the blocks of PMSM drive that have been created or develop to perform in this process which is PI controller, inverse park transformation, SVPWM, park

transformation, clarke transformation and back-EMF estimator block. Figures below shows the a parts of block that have used in simulation process.

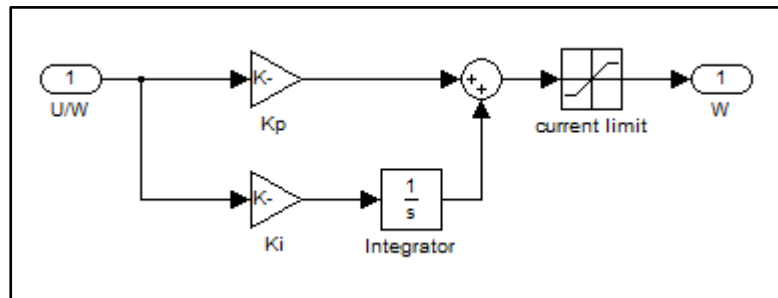


Figure 3.5: PI controller block

From Figure 3.5, the equations for PI controller blok are:

$$U(t) = K_p e + K_i \int e(dt) \quad (3.3)$$

The combination of proportional and integral terms is important to increase the speed of the response and also to eliminate the steady state error. K_p and K_i are the tuning knobs, are adjusted to obtain the desired output.

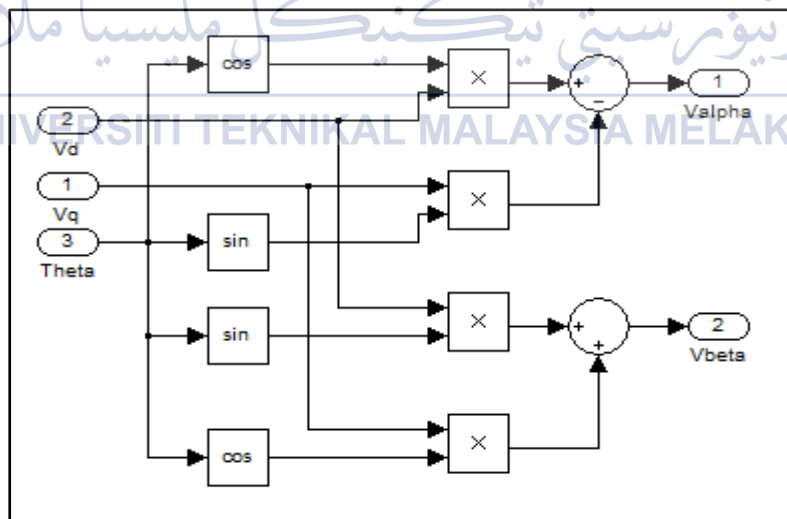


Figure 3.6: Inverse park transformation block

From Figure 3.6, the equations for inverse park transformation blok are:

$$V_{\alpha} = V_d \cos\theta - V_q \sin\theta \quad (3.4)$$

$$V_{\beta} = V_d \sin\theta + V_q \cos\theta \quad (3.5)$$

The outputs of the PI controllers provide the voltage components in the rotating reference frame. Thus an inverse of the previous process has to be applied to get the reference voltage waveforms in a stationary reference frame.

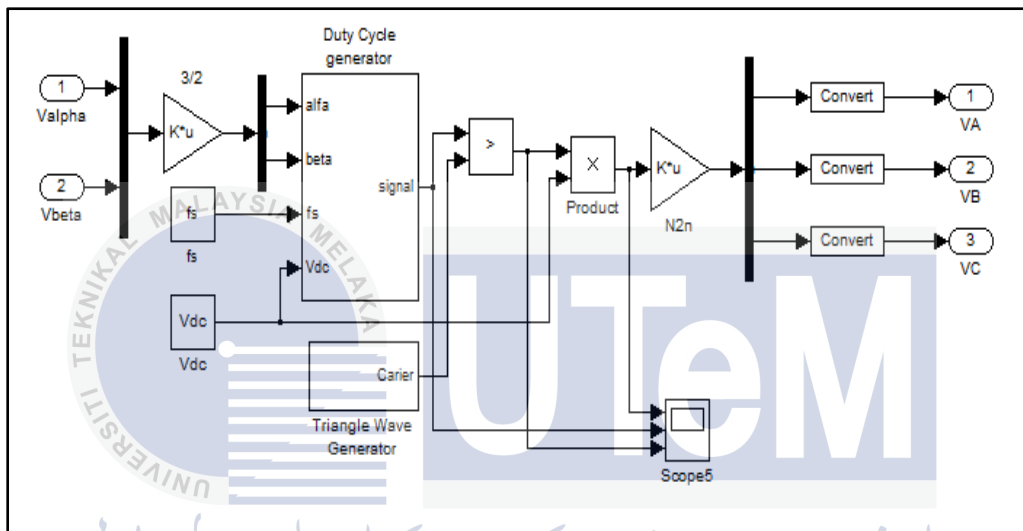


Figure 3.7: SVPWM block

SVPWM is actually just a modulation algorithm which translates phase voltage which is phase to neutral references. Its coming from the controller into modulation times or duty-cycles to be applied to the PWM peripheral. It is a general technique for any three-phase load. Although it has been developed for motor control. SVPWM maximizes DC bus voltage exploitation and uses the "nearest" vectors, which is translates into a minimization of the harmonic content.

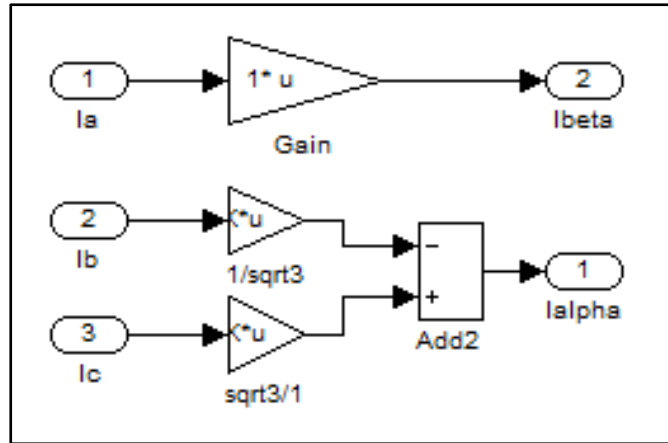


Figure 3.8: Clarke transformation block

From Figure 3.8, the equations for clarke transformation blok are:

$$i_{sa} = i_a \tag{3.6}$$

$$i_{s\beta} = (i_a + 2i_b)/\sqrt{3} \tag{3.7}$$

Clarke transformation is a mathematical transformation employed to simplify the analysis of three-phase circuits. Conceptually it is similar to the dqo transformation. One very useful application of the clarke transformation is the generation of the reference signal used for space vector modulation control of three-phase inverters.

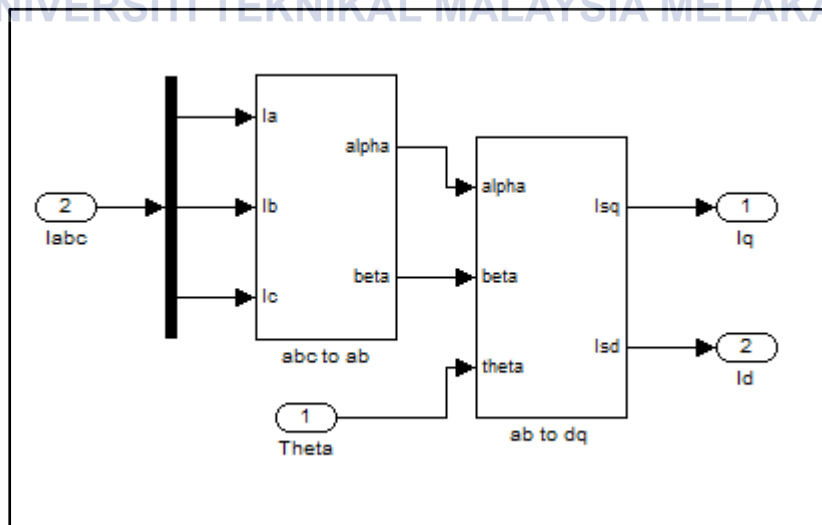


Figure 3.9: Park transformation block

From Figure 3.9, the equations for park transformation blok are:

$$\begin{bmatrix} u_\alpha \\ u_\beta \\ u_0 \end{bmatrix} = \begin{bmatrix} \cos(\omega t) & -\sin(\omega t) & 0 \\ \sin(\omega t) & \cos(\omega t) & 0 \\ 0 & 0 & 1 \end{bmatrix} \cdot \begin{bmatrix} u_d \\ u_q \\ u_0 \end{bmatrix} \quad (3.8)$$

$$i_{sd} = i_{s\alpha} \cos\theta + i_{s\beta} \sin\theta \quad (3.9)$$

$$i_{sq} = -i_{s\alpha} \sin\theta + i_{s\beta} \cos\theta \quad (3.10)$$

Park transformation is a mathematical transformation that rotates the reference frame of three-phase systems in an effort to simplify the analysis of three-phase circuits. In the case of balanced three-phase circuits, application of the *dqo* transform reduces the three AC quantities to two DC quantities. Simplified calculations can then be carried out on these DC quantities before performing the inverse transform to recover the actual three-phase AC results. It is often used in order to simplify the analysis of three-phase synchronous machines or to simplify calculations for the control of three-phase inverters.

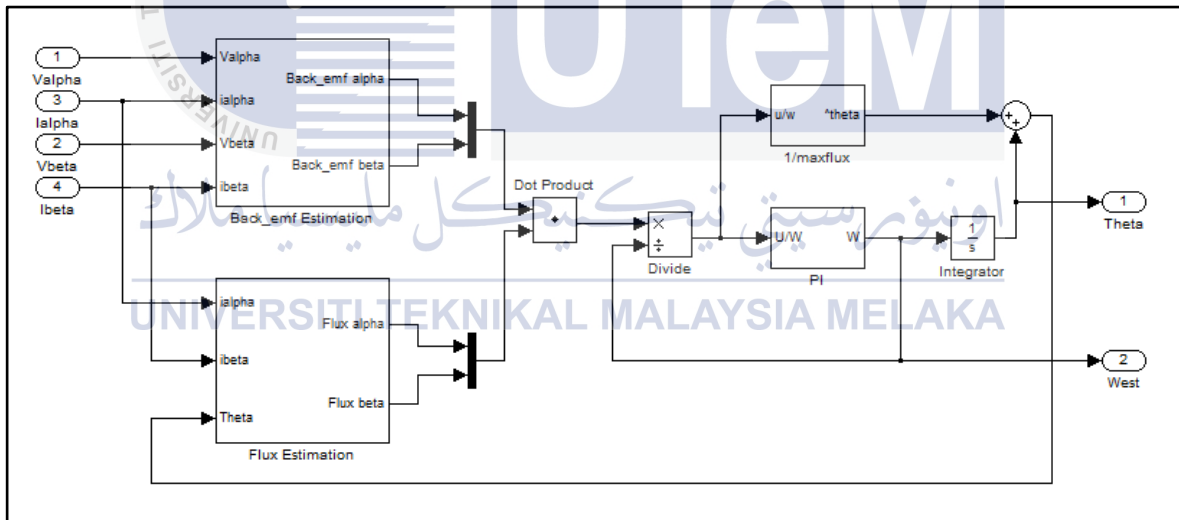


Figure 3.10: Back-EMF estimator block

Figure 3.10 shows the modelling of back-EMF for sensorless PMSM drive. The back-EMF which is calculated based of the voltage and current measurements, is supposed to be accurate and then contains the actual position. By using Equation 3.1 and 3.2 PMSM in the stationary frame was modelled.

To estimate the flux vector the equations is:

$$\begin{aligned}\Psi_{\alpha} &= Li_{\alpha} + \phi_m \cos\theta \\ \Psi_{\beta} &= Li_{\beta} + \phi_m \sin\theta\end{aligned}\quad (3.11)$$

The dot product of the EMF and flux should be permanently equal to zero. However, a residual quantity will appear due to the position estimation error. For small variations about the actual angle the dot product equation is:

$$\Delta\theta = \theta - \hat{\theta}\quad (3.12)$$

Equation 3.12 shows the any error in the position estimation could be removed by keeping the product of back-EMF and flux estimation to be zero. This is achievable by forcing a flux at right angle to the back-EMF through an acceleration or deceleration of the flux vector. A PI controller in this block is used for this purpose.

Fourth phase:

Analysis had been performed when the simulation process has already completed. Ensure the result of the simulation is correct. Troubleshoot process can help to solve the problem when simulation is failing to function properly due to wrong parameters or wrong calculation is used.

Basically, in this phase is a process where analysis for this research will be conducted. So, futher explanation for this process will be provided at the next chapter.

Fifth phase:

Analyzed the result of the simulation. After that, make a report based on the work that has been done for the project. Make sure all objectives of this project are achieved.

CHAPTER 4

RESULT AND DISCUSSION

4.1 Introduction

This chapter will indicate and provide information about the finding of the research, and all the finding will be analyzed and discussed. This chapter will discuss more on the process of analyzing the result from the stage of how the research had been conducted until the process of data comparison validation process.

The simulation process is performed to finding the position and speed estimation based on back-EMF sensorless control for PMSM using SIMULINK/MATLAB software. The technique that had been used to control the drive system is field oriented control (FOC) or vector control. From the motor drive system, the estimator of speed and position motor is used to estimate the speed and position of the motor. The result shows the difference in speed, which is actual speed and speed estimator. The results of currents from the motor drive also will be shown in this chapter.

4.2 Simulation of PMSM Using Back-EMF Sensorless Control

After has been reviewed about the PMSM using back-EMF sensorless control, the simulation progress can be constructed. The overall simulation block diagram the PMSM using back-EMF sensorless control in Figure 4.1 consists of speed controller (PI), current controller (PI), SVPWM, voltage source inverter (VSI), bus selector parameters, PMSM model, current transformation, voltage transformation and estimator using back-EMF technique.

There are some parameters of the motor are used which is PMSM drive to modelled this simulation as shown in Table 4.1.

Table 4.1: Parameter of induction motor

Section	Specification of Motor	Details
General	Type of Motor	PMSM drive
	Model No.	BSM90C-2150
	Continuous Torque	5.2 N.m
	Continuous Current	4.78 A
	Peak Torque	138.1 N.m
	Peak Current	12.2 A
	Thermal Resistance	0.9 °C/Watt
	Thermal Time constant	45 min
	Mechanical Time Constant	2.32 m sec
	Electrical Time Constant	2.96 m sec
	Rated Speed at 300V	2000 rpm
Electrical	Torque Constant	1.38 N.m
	Voltage Constant ($V_{peak}/krpm$)	118.8 V
	Resistance	5 Ω
	Inductance	14.8 mH
Mechanical	Inertia ($kg.cm^2$)	0.881 m J
	Max. Speed	10000 rpm
	No. Of Poles Pair	4
	Weight (lbs/kg)	23/10.5

4.3 Back-EMF Observer

In this simulation the voltage and current outputs of the induction machine PMSM model are used to be an estimator on back-EMF. The observers are configured to estimate the components of back-EMF. The error between the outputs of the observers is used to derive a suitable adaptation mechanism which generates the estimated speed of the adaptive model as shown in Figure 4.2. In Figure 4.2, the adaptive model is configured based on Figure 2.11 and similarly the reference model is configured according to Equation 2.26 and Equation 2.29 that have been discussed in chapter two.

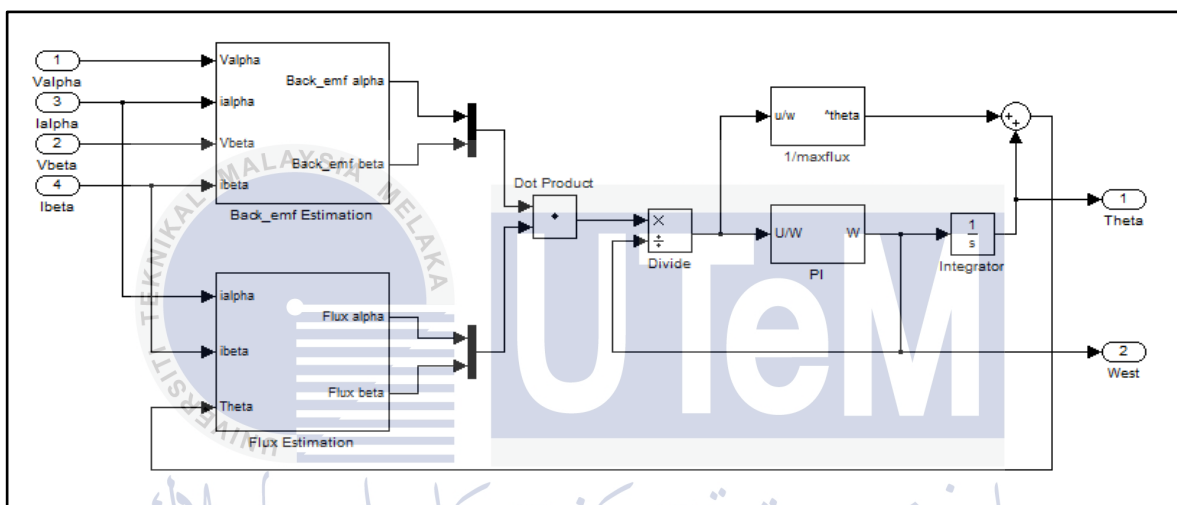


Figure 4.2: Estimator block diagram in simulation

4.4 Result Of Simulation

From Table 4.1, the PMSM parameter is used to perform this experiment to get the expected result. The result shows three conditions which is, in full rated speed the motor will test at 209 rad/s, meanwhile at half rated speed the motor will test at 105 rad/s and lastly at low rated speed the motor will test at 31 rad/s. These three conditions of the experiment is tested again with load disturbance in the system. The load disturbance of 1 N.m will apply at $t = 3$ seconds during the motor running. The result shown in rad/s unit due to the system under this experiment is placed a conversion from the rpm unit to rad/s unit. The experimental range of speed, with load and without load is performed under the

rated speed and load given. All results of the graphs will be shown below in zoom on each step response shows in the graphs for more details.

From the result, the discussion will be perform to find out the performance of the PMSM system with estimator method which is back-EMF sensorless technique. The information of graphical result can be analyzed. There is an overshoot, undershoot, steady state rise time and settling time. From this information the performance of motor with estimator method are known.

4.4.1 Simulation without load disturbance condition

- i. Condition 1: When reference speed = 209 rad/s and without load condition.

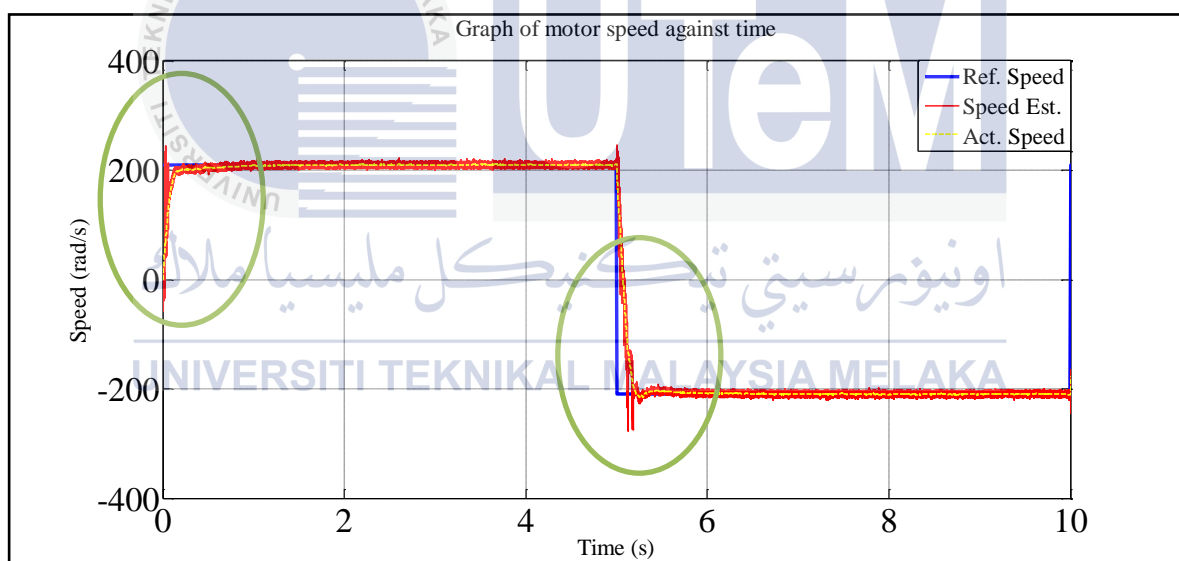


Figure 4.3: Comparison between reference speed, speed estimator and actual speed

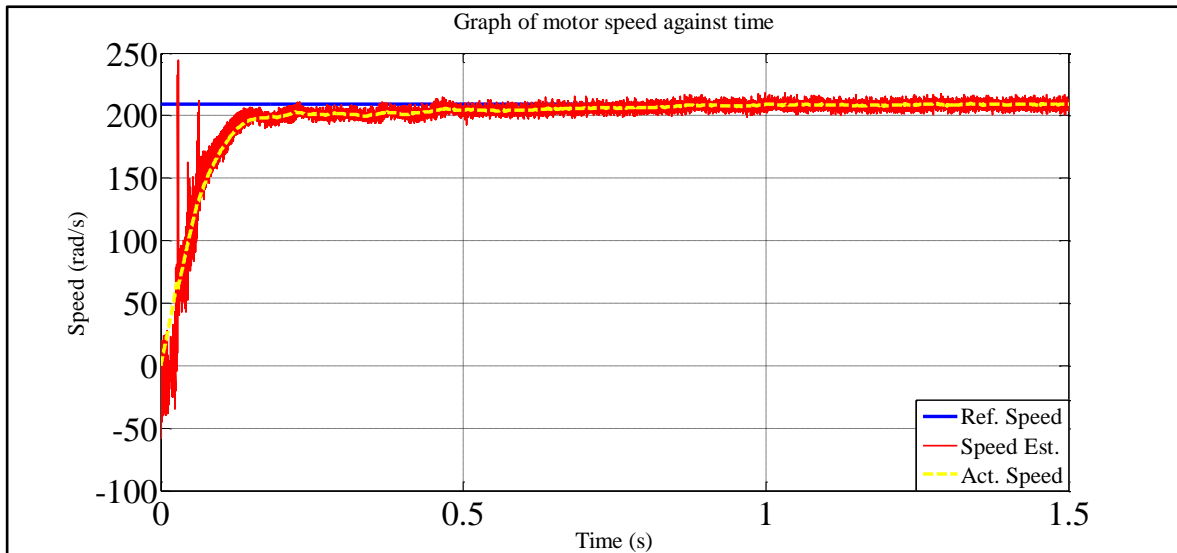


Figure 4.4: Zoom view at starting speed during forward condition

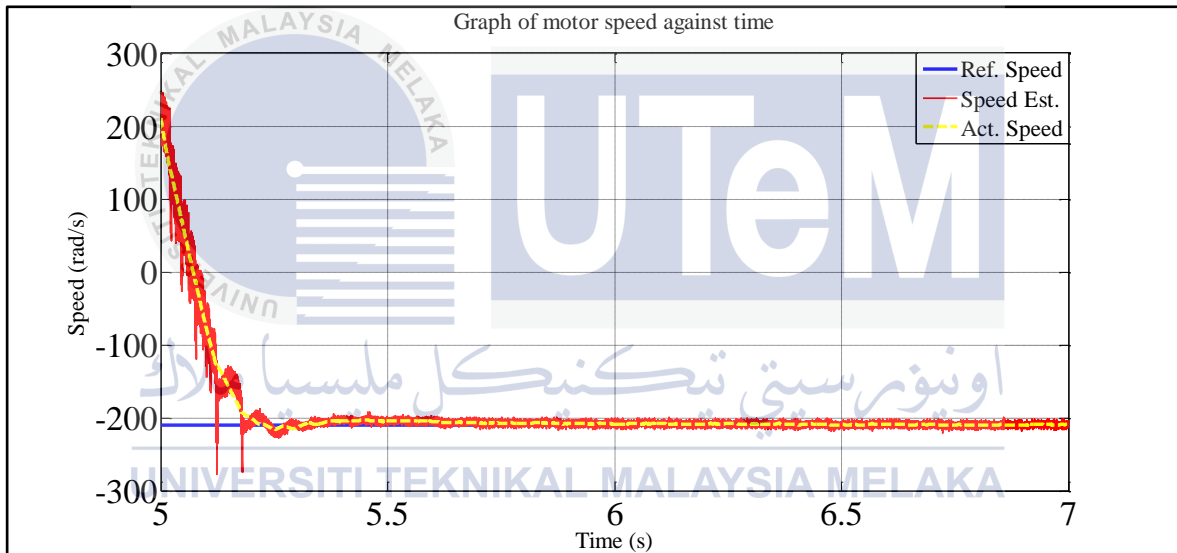


Figure 4.5: Zoom view at starting speed during reverse condition

From the result in the Figure 4.4, the settling time is at $t = 0.48$ seconds and become stable at steady state condition at $t = 0.6$ seconds. Meanwhile, the rise time is at $t = 0.12$ seconds. At $t = 5$ seconds, the undershoot exist due to reverse direction of a motor which shown at Figure 4.5. The undershoot value in percent is 7% from the rated value. This is because of the system are tuned at full rated condition and the system is very stable during the speed in 209 rad/s.

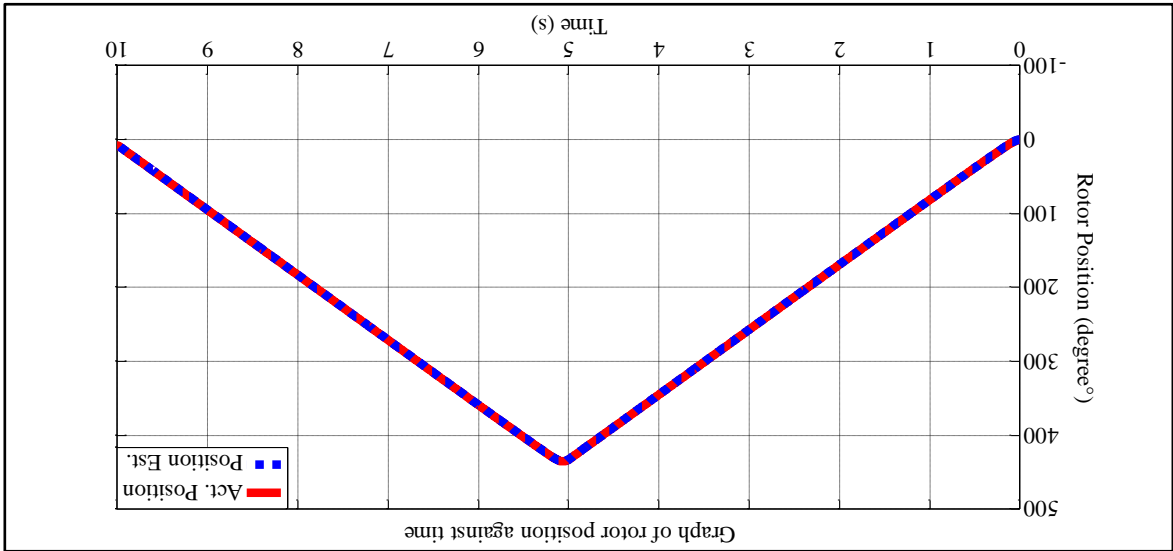


Figure 4.6: Comparison between actual position and position estimator of rotor

For the rotor position angle in the Figure 4.6 shows a comparison between the actual and estimated of rotor position of a motor. This result shows for full rated speed of the rotor position angle is 435°. After in 5 seconds the position of the rotor will turn to reverse direction. This results show doesn't have any problem to estimated a position of the angle rotor with this sensorless method.

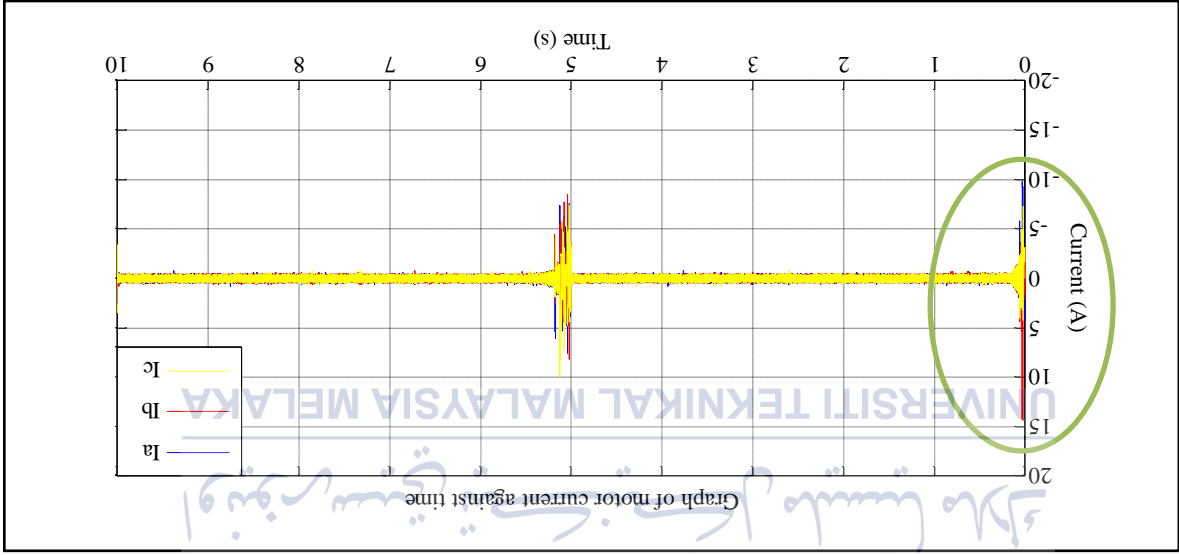


Figure 4.7: Comparison between current I_a , I_b and I_c

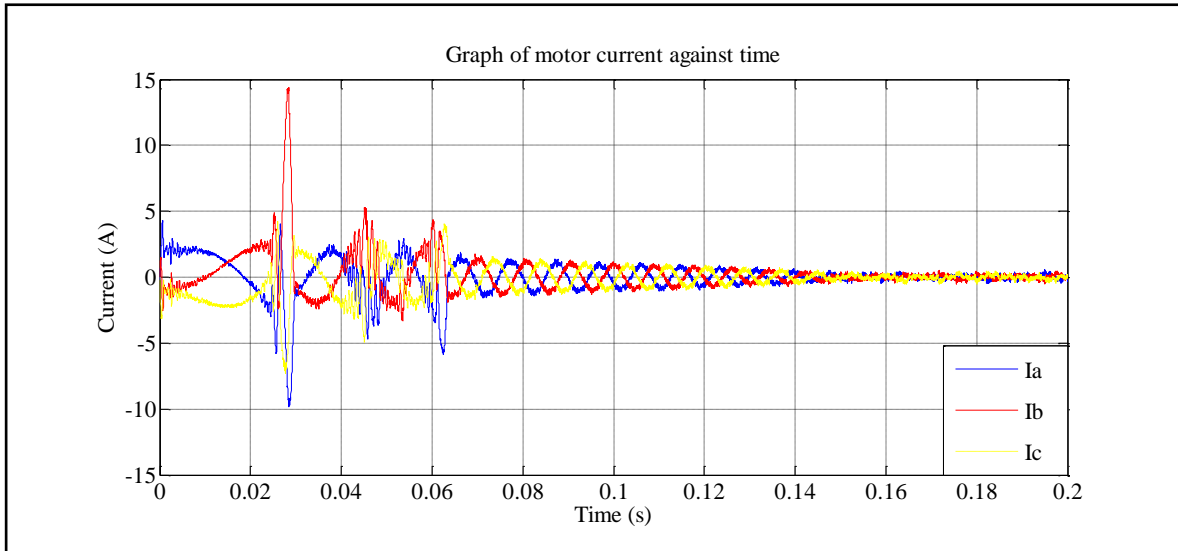


Figure 4.8: Zoom view during the starting current

The phase current I_a , I_b and I_c in Figure 4.8 shows that at the starting point, $t = 0.03$ seconds, current is high due to surge current during start-up of the drive system. The system takes only 0.14 second to make it stable. The phase current also increase of the reverse direction of the motor at $t = 5$ seconds as shown in Figure 4.7.

- ii. Condition 2: When reference speed = 105 rad/s and without load condition.

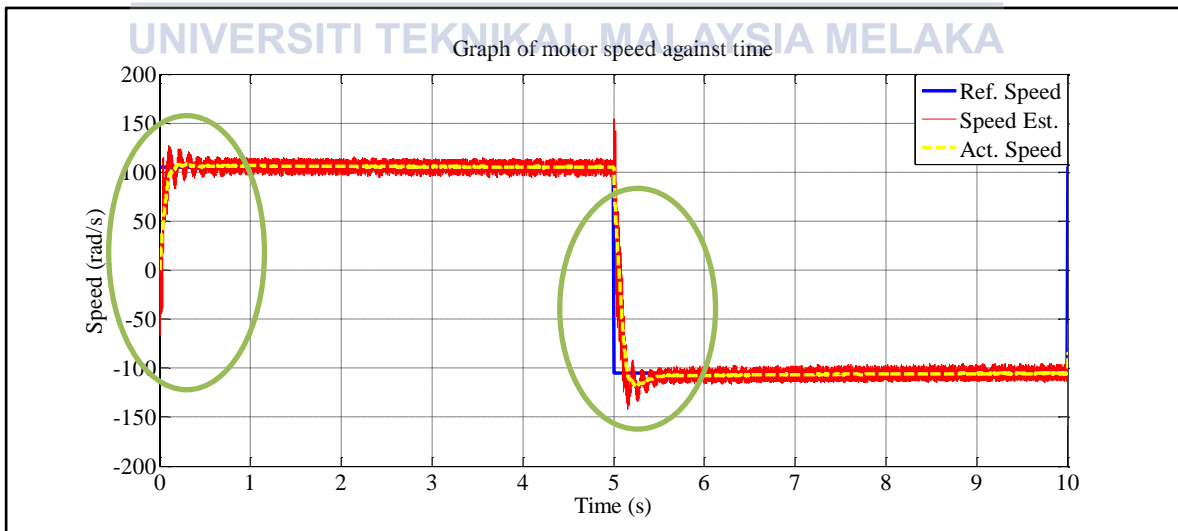


Figure 4.9: Comparison between reference speed, speed estimator and actual speed

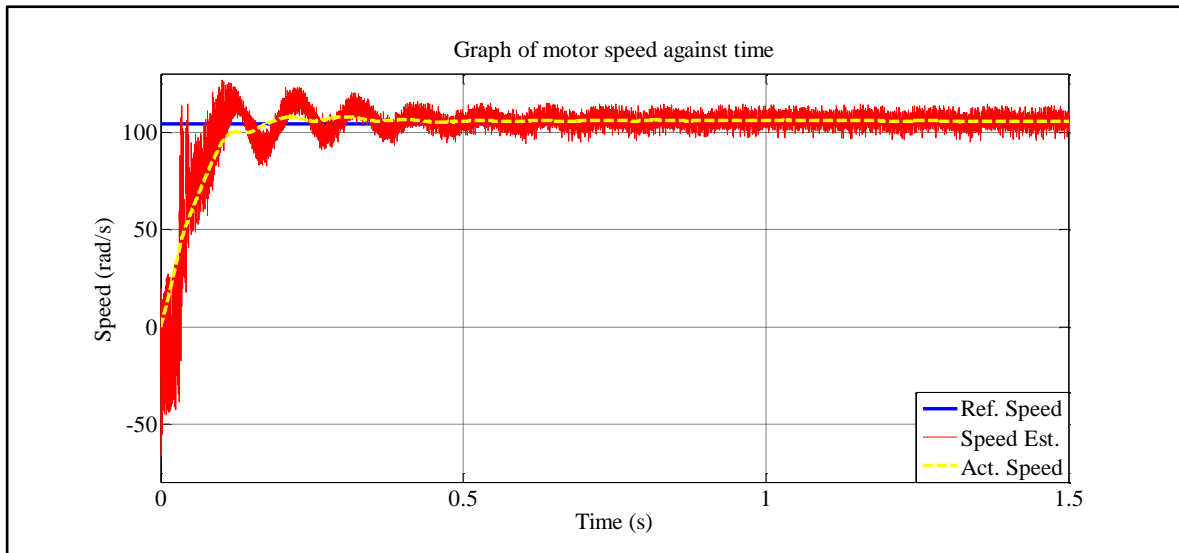


Figure 4.10: Zoom view at starting speed during forward condition

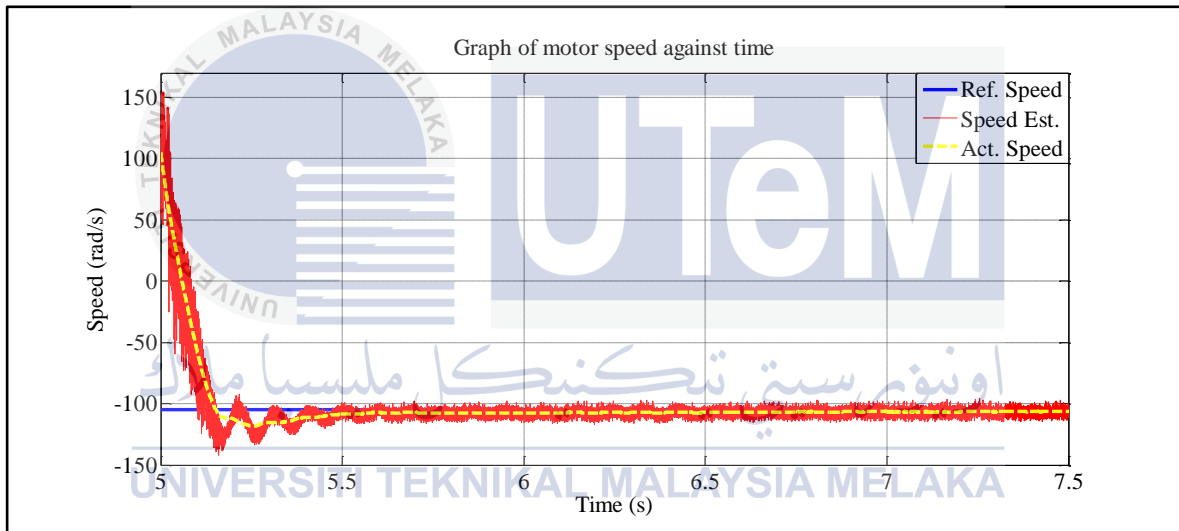


Figure 4.11: Zoom view at starting speed during reverse condition

Based on observation in Figure 4.10, the settling time is $t = 0.5$ seconds and the rise time is at $t = 0.09$ seconds. The system starts to stable at $t = 0.65$ seconds. There is an overshoot at a starting point and an undershoot at the reverse direction of a motor as shown in Figure 4.10 and 4.11. The value of overshoot and undershoot in percent is 16% and 25% respectively. The ripple in a speed estimator of half rated condition shows is higher than the full rated condition because of the controller that used is tuned at full rated condition.

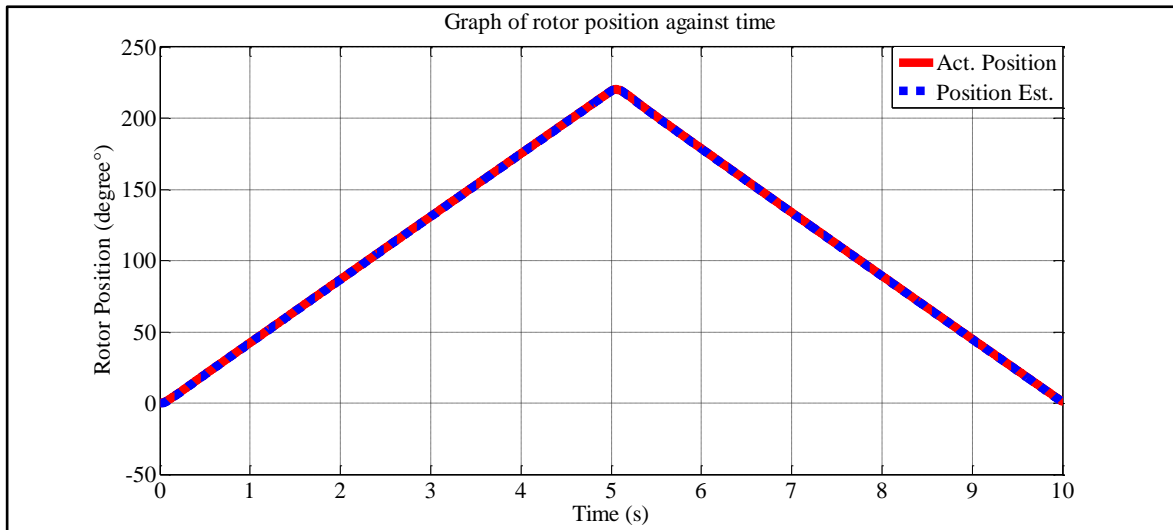


Figure 4.12: Comparison between actual position and position estimator of rotor

For the rotor position angle in the Figure 4.12 shows a comparison between the actual and estimated of rotor position of a motor. This result shows for half rated speed of the rotor position angle is 220° . In half rated speed condition, the result of rotor position in rad/s is represented lower than full rated speed condition. At $t = 5$ seconds the position of the motor will turn to reverse direction. This results show doesn't have any problem to estimated a position of the angle rotor with this sensorless method.

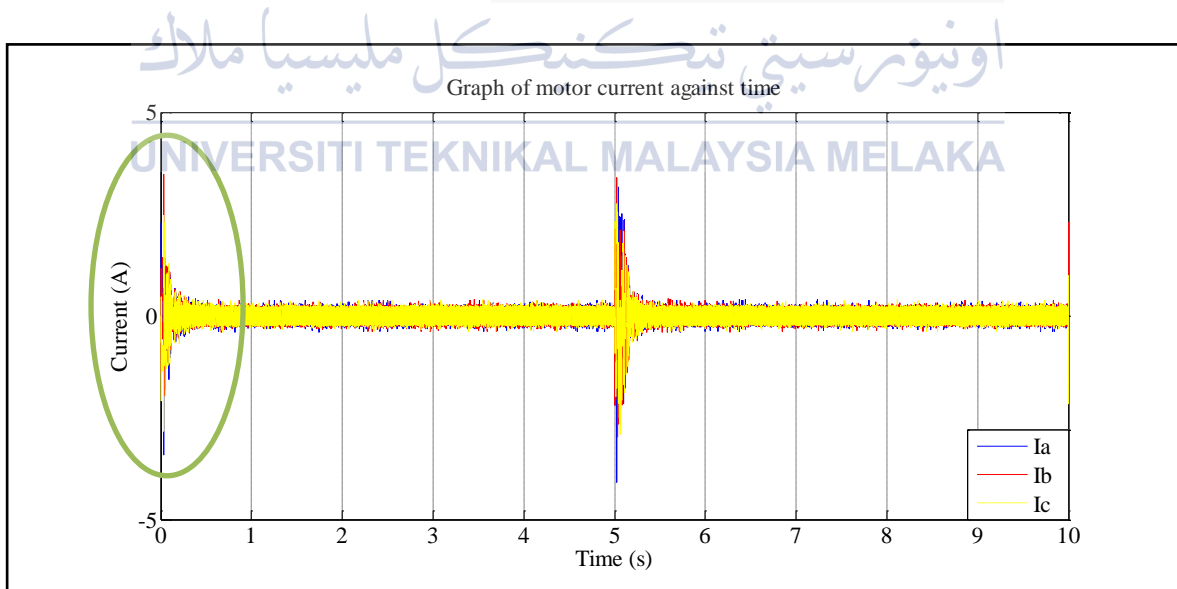


Figure 4.13: Comparison between current I_a , I_b and I_c

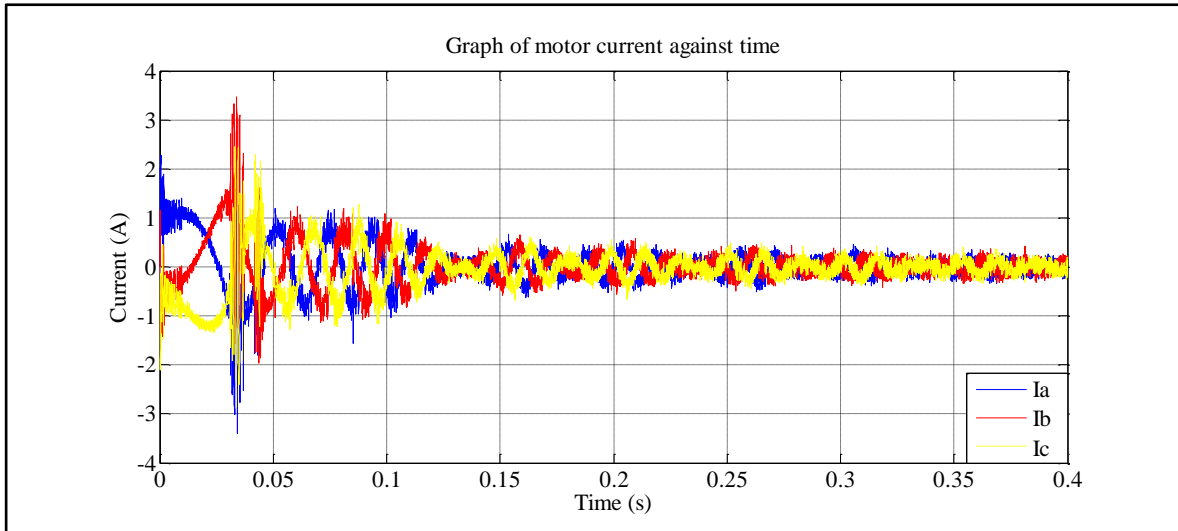


Figure 4.14: Zoom view during the starting current

The phase current I_a , I_b and I_c in Figure 4.14 shows that at a starting point, $t = 0.038$ seconds, current is high due to surge current during start-up of the drive system. The system takes 0.3 seconds to make it stable. The phase current also increase of the reverse direction at $t = 5$ seconds of the motor as shown in Figure 4.13.

- i. Condition 3: When reference speed = 31 rad/s and without load condition.
- ii.

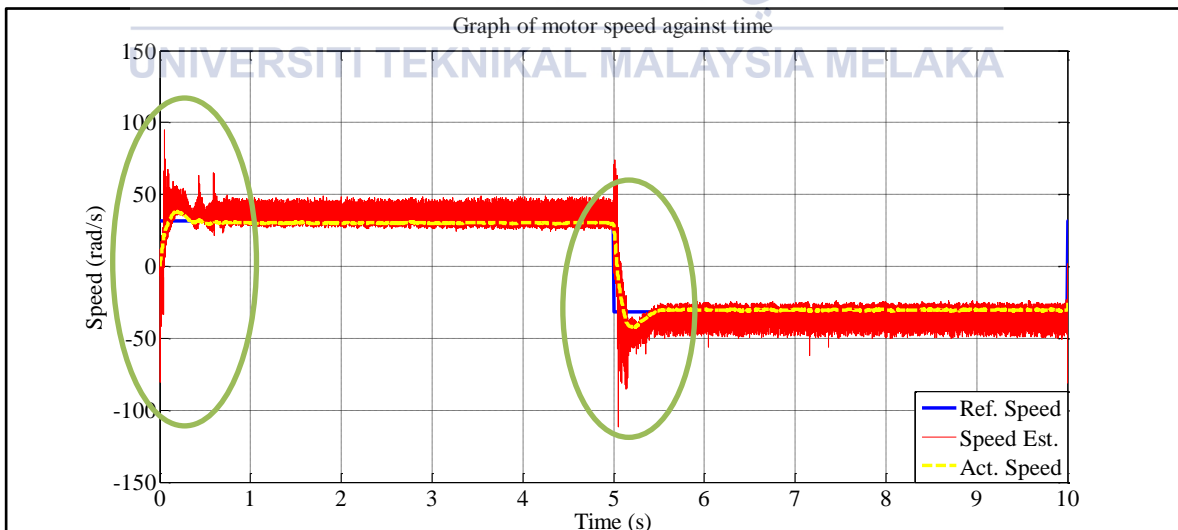


Figure 4.15: Comparison between reference speed, speed estimator and actual speed

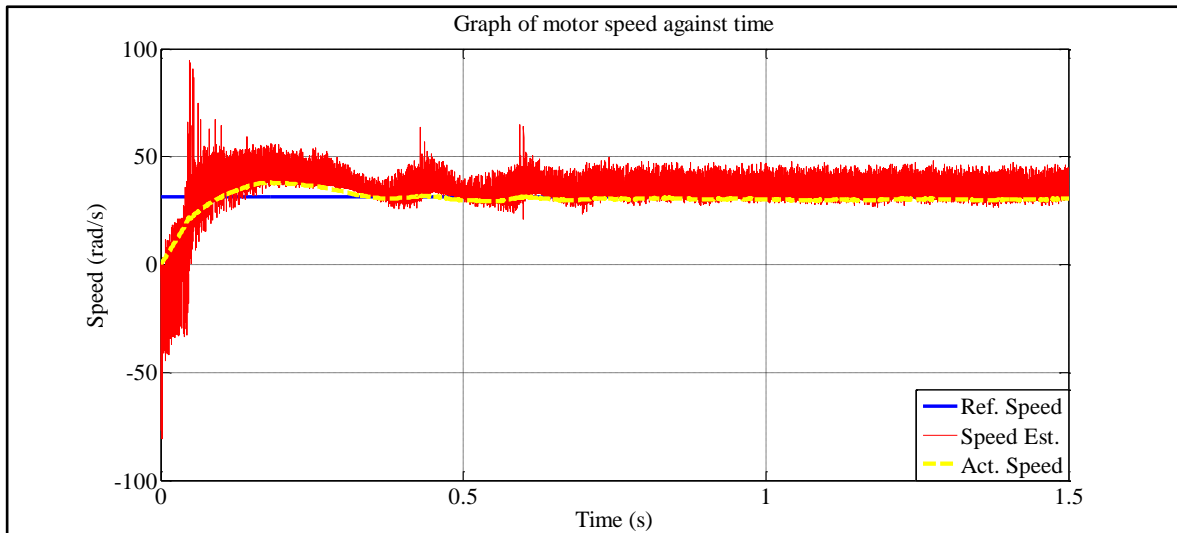


Figure 4.16: Zoom view at starting speed during forward condition

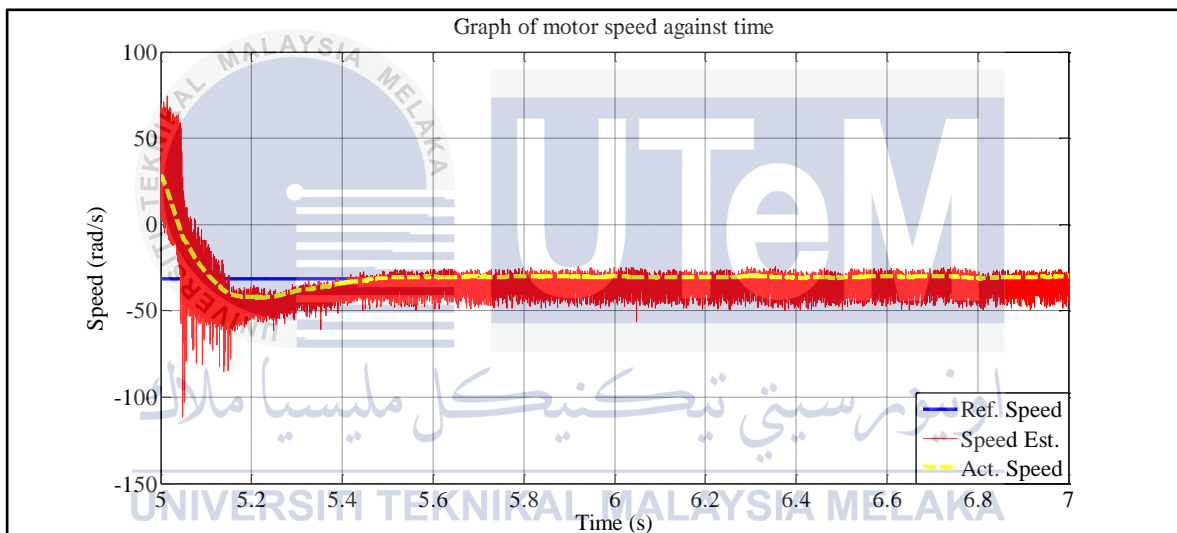


Figure 4.17: Zoom view at starting speed during reverse condition

In Figure 4.16, the settling time is $t = 0.62$ seconds and the rise time is at $t = 0.07$ seconds. The system starts to stable at $t = 0.78$ seconds. There is an overshoot at a starting point and an undershoot at the reverse direction of a motor as shown in Figure 4.16 and 4.17. The value of overshoot and undershoot in percent is 60% and 67% respectively from the rated value. The ripple in a speed estimator of half rated condition showed is higher than the full and half rated condition because of the controller that used is tuned at full rated condition. Where the low rated speed condition is unstable in this system compare with full and half rated speed.

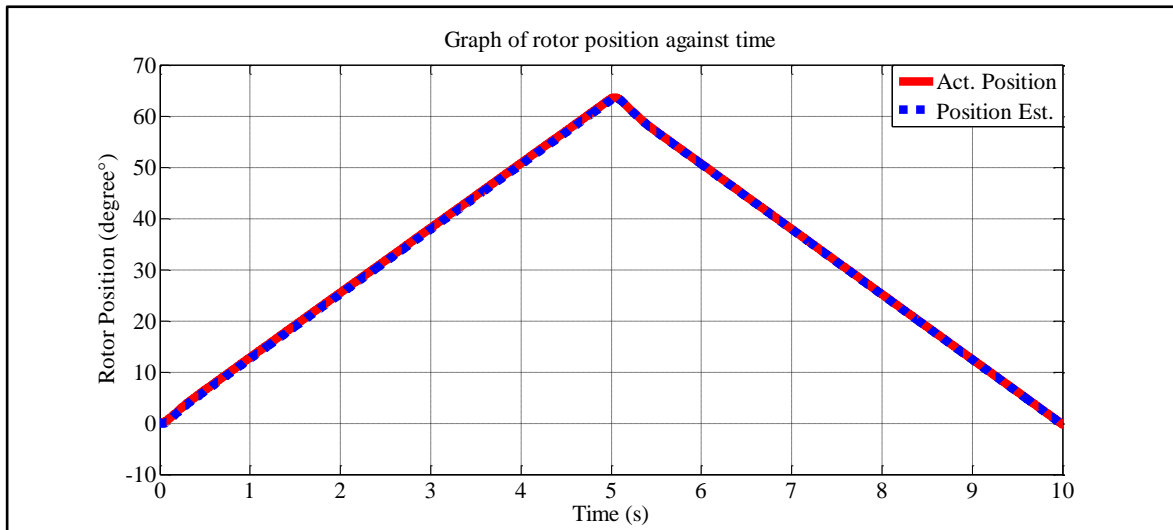


Figure 4.18: Comparison between actual position and position estimator of rotor

For the rotor position angle in the Figure 4.18 shows a comparison between the actual and estimated of rotor position of a motor. Found that, not much difference angle of the rotor position between actual and estimated results of those tested. This result shows for low rated speed of the rotor position angle is 63° . In low rated speed condition, the result of rotor position in rad/s is represented lower than full and half rated speed condition. At $t = 5$ seconds the motor will turn to reverse direction. This results show doesn't have any problem to estimated a position of the angle rotor with this sensorless method.

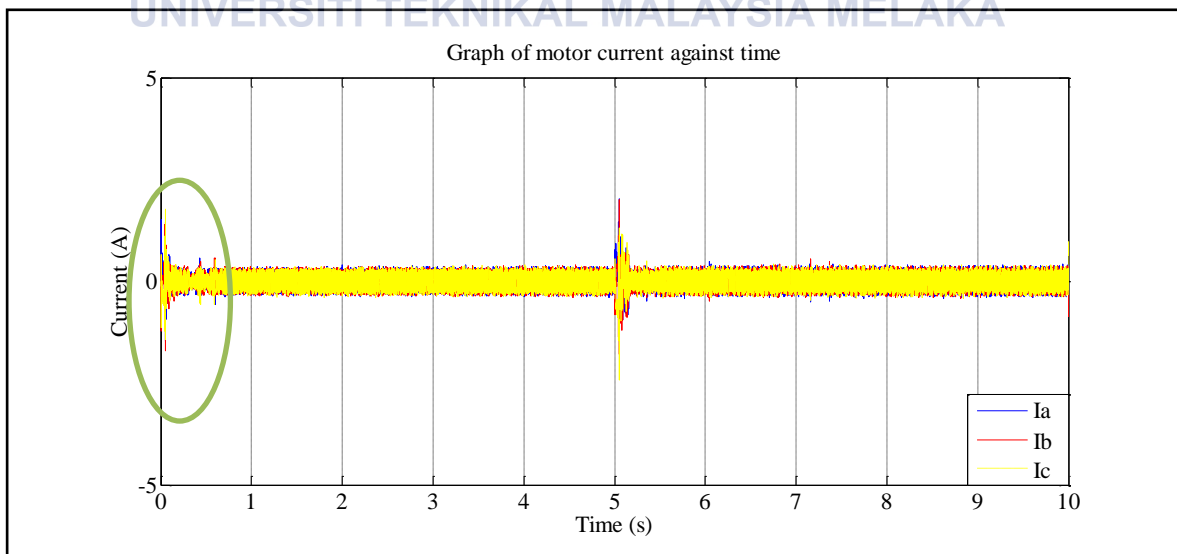


Figure 4.19: Comparison between current I_a , I_b and I_c

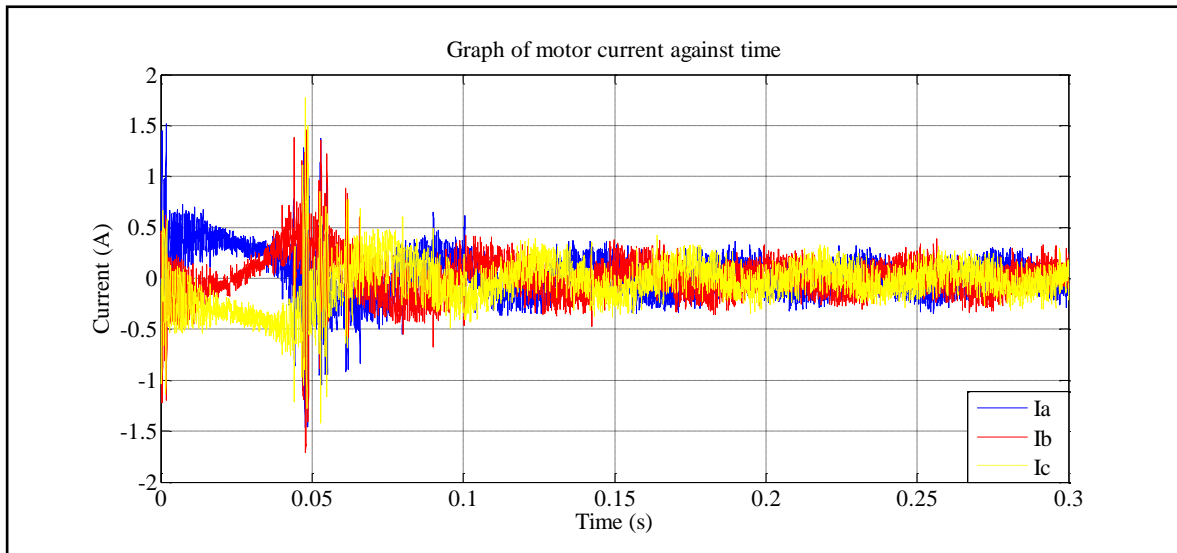


Figure 4.20: Zoom view during the starting current

The phase current I_a , I_b and I_c in Figure 4.20 shows that at a starting point, $t = 0.047$ seconds, current is high due to surge current during start-up of the drive system. The system only takes 0.16 seconds to make it stable. The phase current also increase of the reverse direction at $t = 5$ seconds of the motor as shown in Figure 4.19.

4.4.2 Simulation with load disturbance condition

- i. Condition 1: When reference speed = 209 rad/s and step load torque at $t = 3$ seconds under 1 N.m.

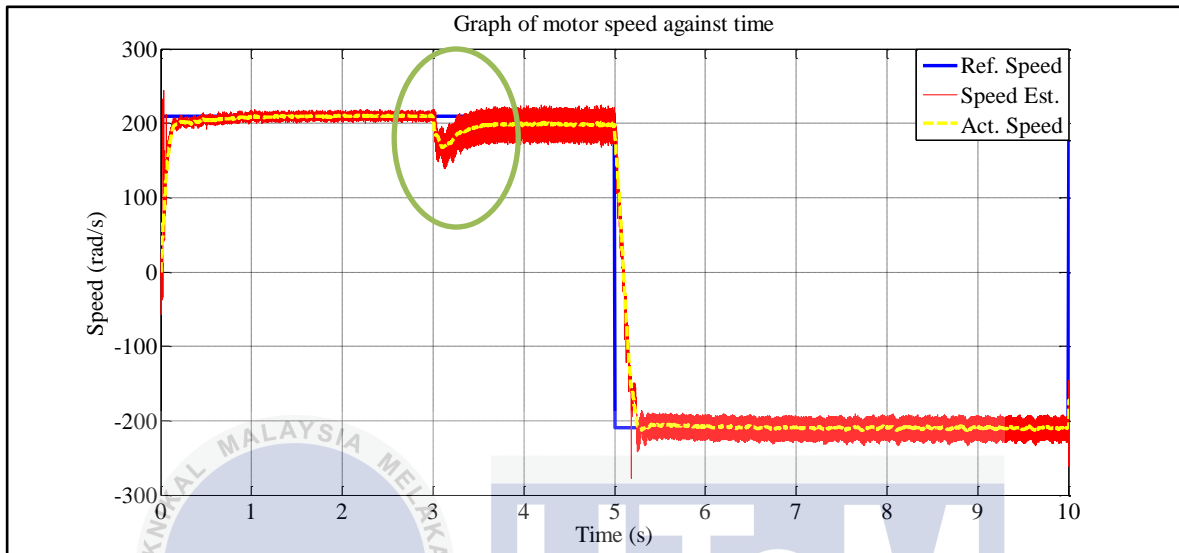


Figure 4.21: Comparison between reference speed, speed estimator and actual speed with load disturbance

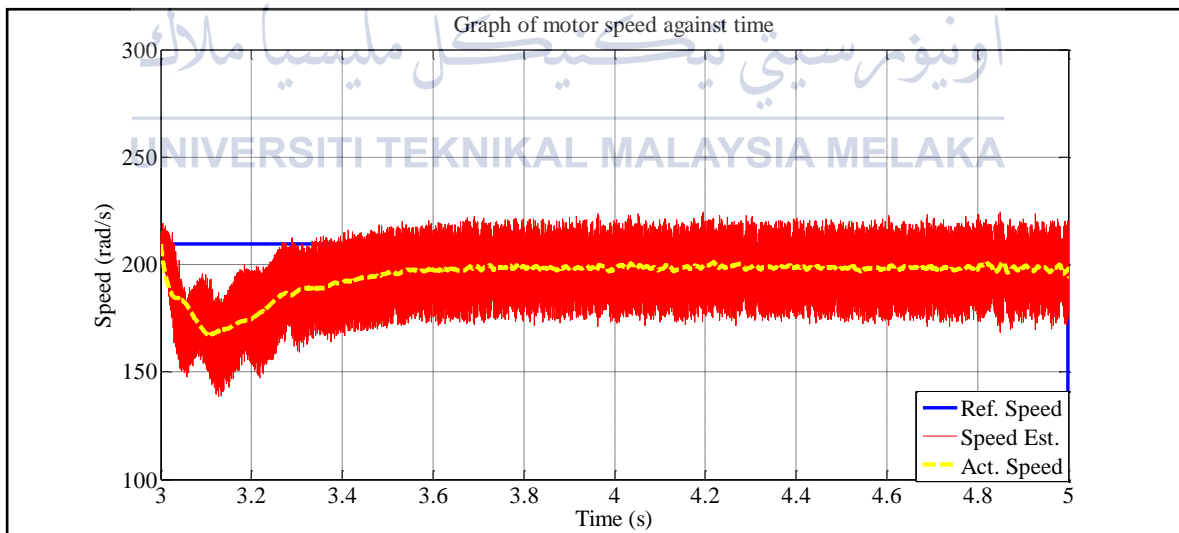


Figure 4.22: Zoom view of speed during load disturbance

In the Figure 4.21 shows in time, when $t = 3$ seconds, sudden application of a 1 N.m load disturbance, when the motor run at 209 rad/s. There is having an undershoot at this point. The undershoot is in 69% from the rated value. The recovery time is at $t = 3.6$ seconds and become stable at steady state condition after load disturbance occurred. In a load disturbance condition, the speed estimator increase around 73% from no load condition rated.

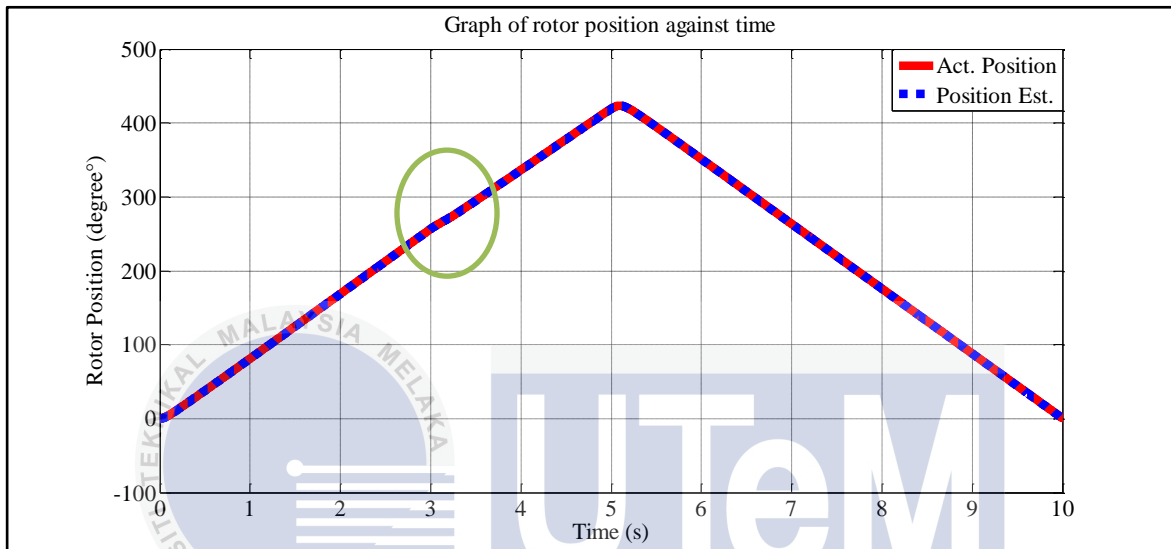


Figure 4.23: Comparison between actual position and position estimator of rotor with load disturbance

For the rotor position angle in the Figure 4.23 shows a comparison between the actual and estimated of rotor position of a motor during sudden application of a 1 N.m load disturbance. The graph shown have a very small curve at $t = 3$ seconds due to load disturbance occurred. This result shows the rotor position angle is 423° . At $t = 5$ seconds the position of the rotor will turn to reverse direction. This result shows doesn't have any problem to estimated a position of the angle rotor with this sensorless method.

For the phase current I_a , I_b and I_c in Figure 4.25 shows at a load disturbance point, $t = 3$ seconds, current become higher due to load torque occurred. The system become stable at $t = 3.12$ seconds. The current increase in 75% from no load condition rated.

Figure 4.25: Zoom view during the starting current at load disturbance

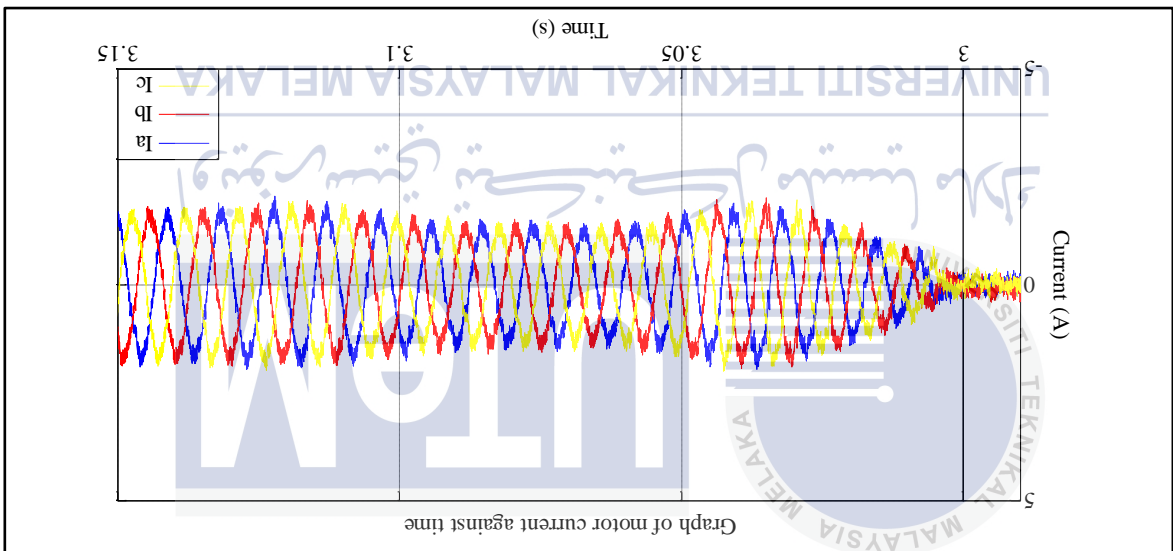
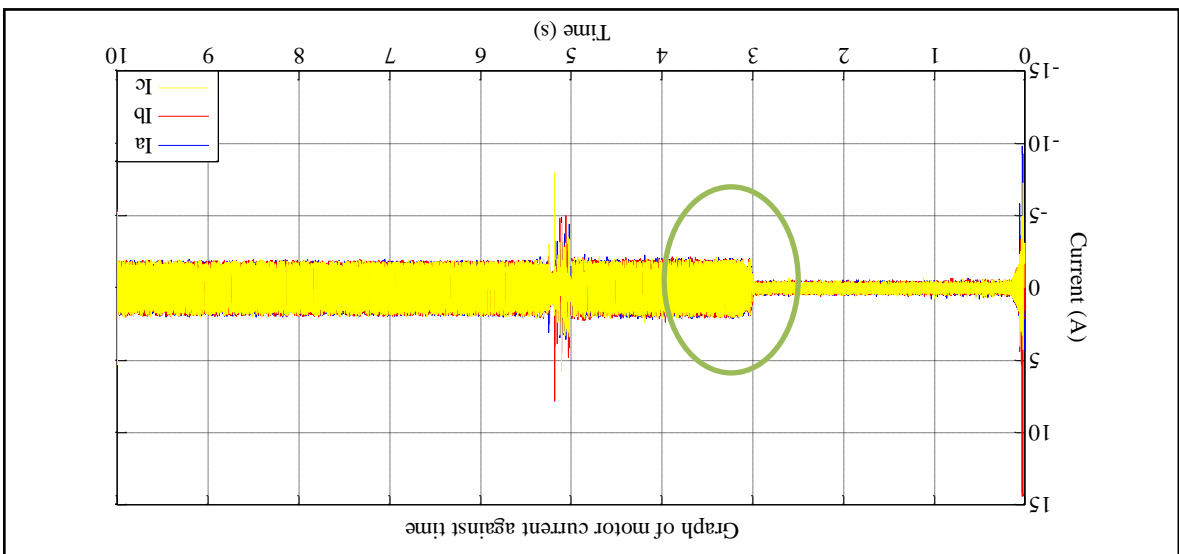


Figure 4.24: Comparison between current I_a , I_b and I_c



- ii. Condition 2: When reference speed = 105 rad/s and step load torque at $t = 3$ seconds under 1 N.m.

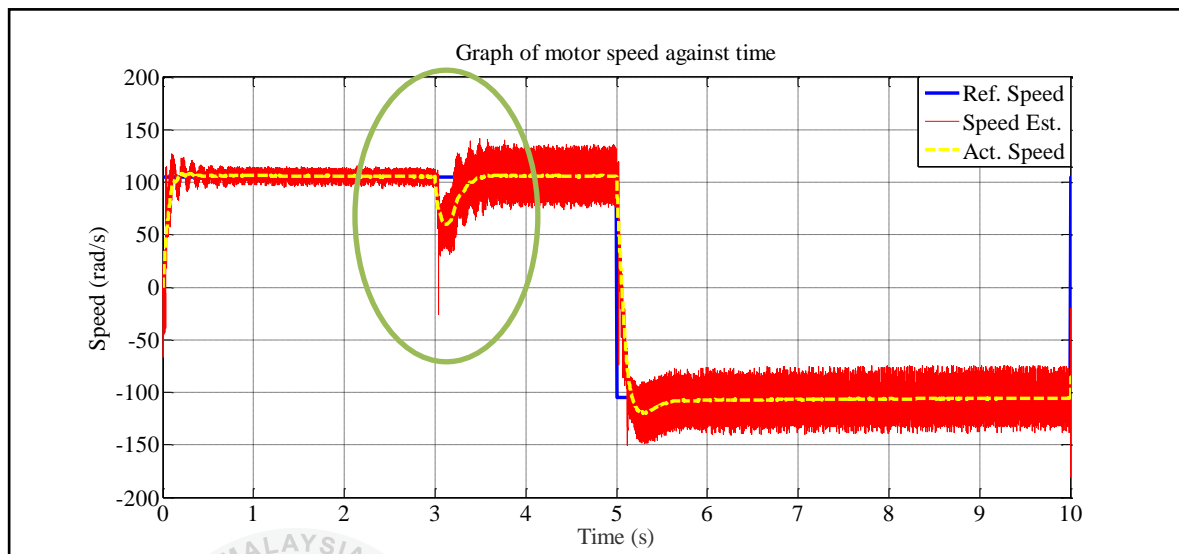


Figure 4.26: Comparison between reference speed, speed estimator and actual speed with load disturbance

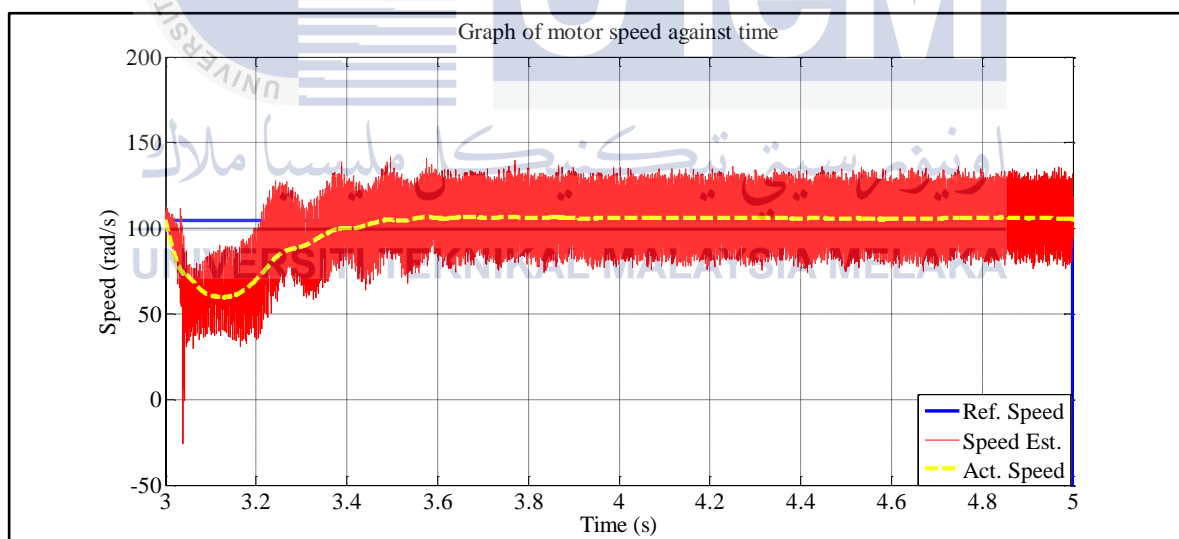


Figure 4.27: Zoom view of speed during load disturbance

From the Figure 4.26 shows in time, when $t = 3$ seconds, sudden application of a 1 N.m load disturbance occurred during the motor run at 105 rad/s. There is having an undershoot at this point. The undershoot is in 57% from the rated value. The recovery time is at $t = 3.5$ seconds, and become stable at steady state condition after load disturbance

occurred. In a load disturbance condition, the speed estimator increase in 75%. From this result, the speed estimator is higher than the speed estimator of full rated condition.

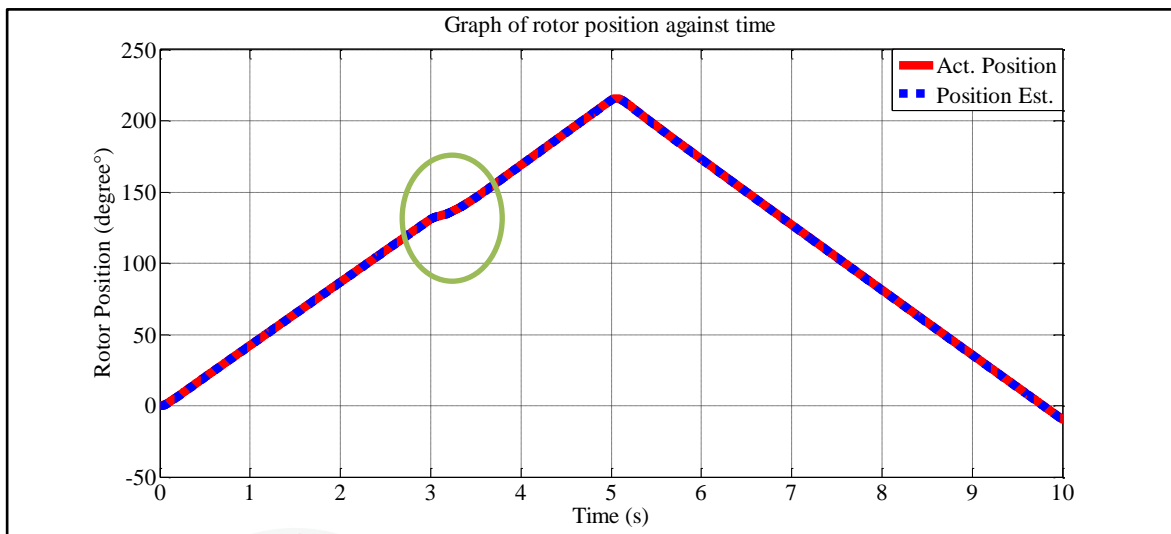


Figure 4.28: Comparison between actual position and position estimator of rotor with load disturbance

For the rotor position angle in the Figure 4.28 shows a comparison between the actual and estimated of rotor position of a motor during sudden application of a 1 N.m load disturbance. The graph shows have a small curve at $t = 3$ seconds due to load disturbance occurred. This result showed for the half rated speed of the rotor position angle is 216° . At $t = 5$ seconds the position of the rotor will turn to reverse direction. The result of rotor position in rad/s was represented lower than full rated speed condition. This result shows doesn't have any problem to estimated a position of the angle rotor with this sensorless method.

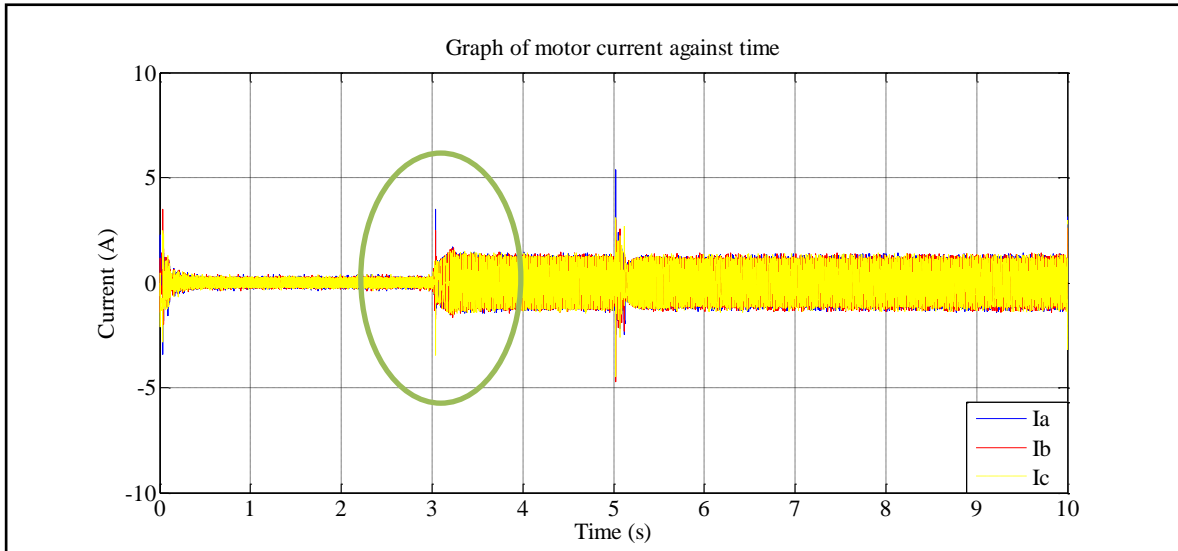


Figure 4.29: Comparison between current I_a , I_b and I_c with load disturbance

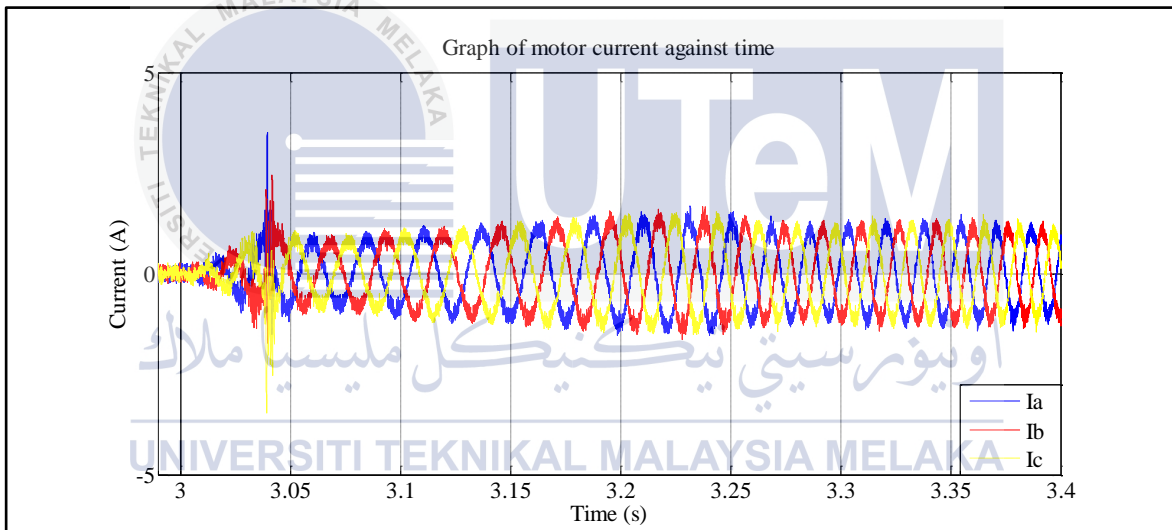


Figure 4.30: Zoom view during the starting current at load disturbance

For the phase current I_a , I_b and I_c in Figure 4.30 shows at a load disturbance point, $t = 3$ seconds, current become higher due to load torque occurred. The system become stable at $t = 3.35$ seconds. The current increase in 73% from no load condition rated. In half rated speed condition, current at a starting point and direction change point of a motor is represented lower than full rated speed condition.

iii. Condition 3: When reference speed = 31 rad/s and step load torque at $t = 3$ seconds under 1 N.m.

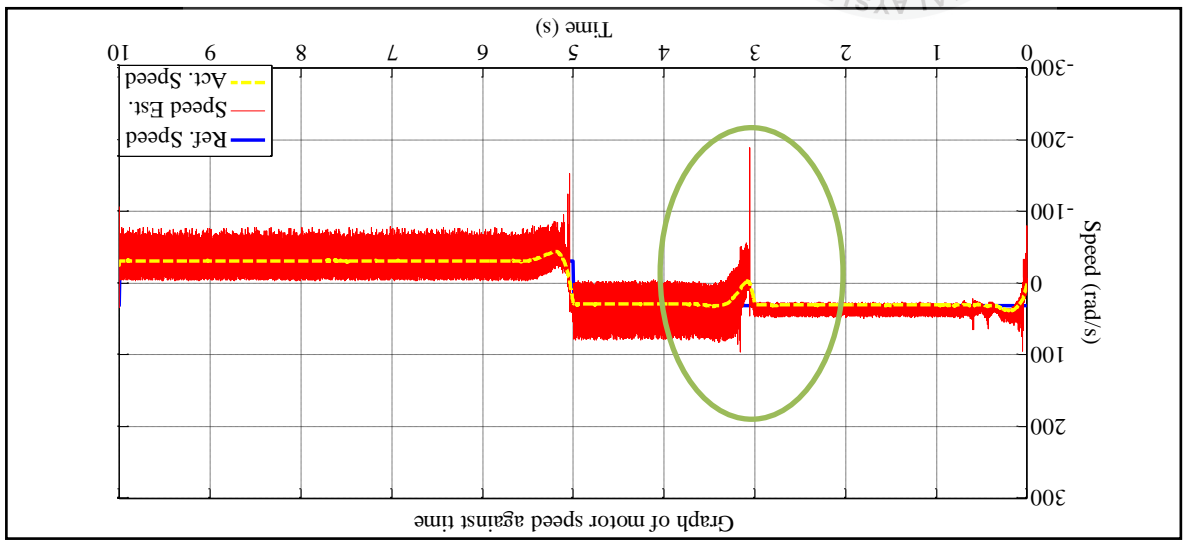


Figure 4.31: Comparison between reference speed, speed estimator and actual speed with load disturbance

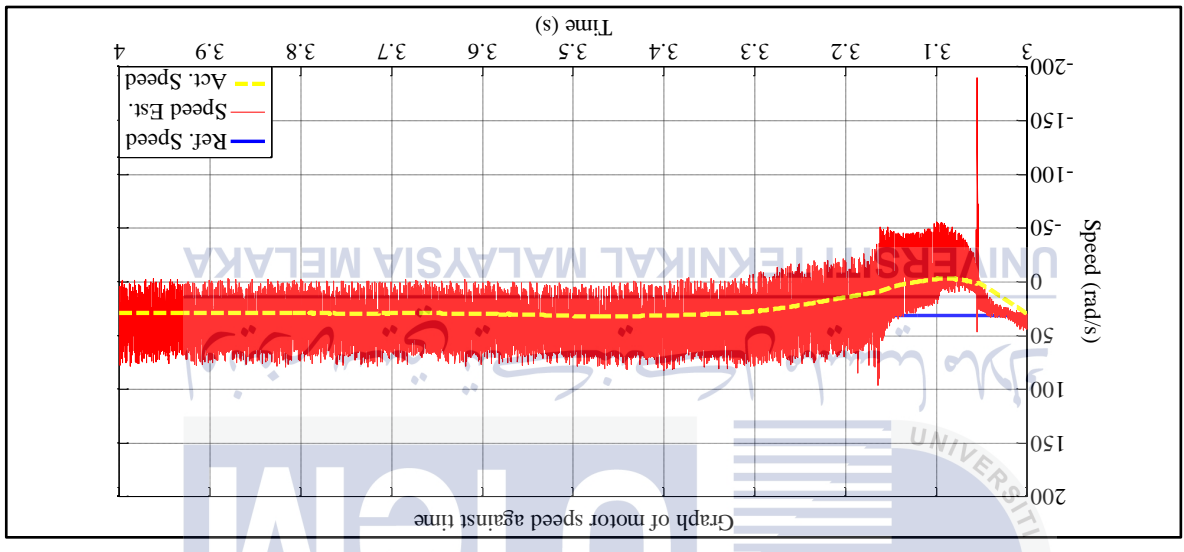


Figure 4.32: Zoom view of speed during load disturbance

From the Figure 4.32 shows, at $t = 3$ seconds, sudden application of a 1 N.m load disturbance occurred when the motor run at 31 rad/s. There is an undershoot at this point. The undershoot is 55% from the rated value. The recovery time for the speed is at $t = 3.4$ seconds and become stable at steady state condition after load disturbance occurred. From

this result, the speed estimator increase in 77%. This result showed the speed estimator is higher than the speed estimator of full and half rated speed condition.

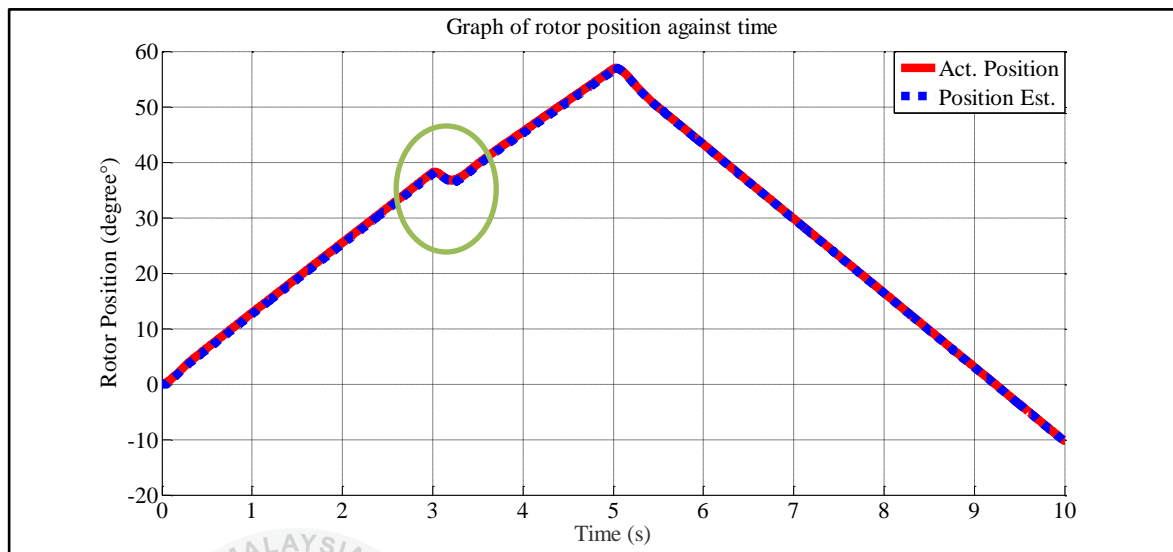


Figure 4.33: Comparison between actual position and position estimator of rotor with load disturbance

For the rotor position angle in the Figure 4.33 shows a comparison between the actual and estimated of rotor position of a motor during sudden application of a 1 N.m load disturbance. The graph shown have a curve at $t = 3$ seconds due to load disturbance occurred. This result showed for low rated speed of the rotor position angle is 57° . At $t = 5$ seconds the position of the rotor will turn to reverse direction. In low rated speed condition, the result of rotor position in rad/s is represented lower than full and half rated speed condition. This result shows doesn't have any problem to estimated a position of the angle rotor with this sensorless method.

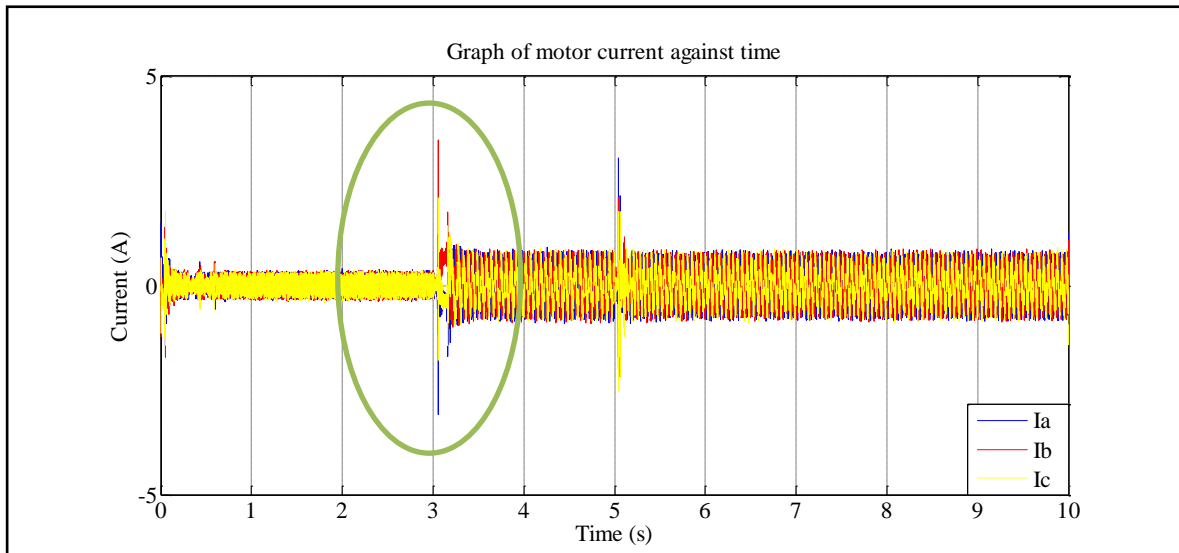


Figure 4.34: Comparison between current I_a , I_b and I_c with load disturbance

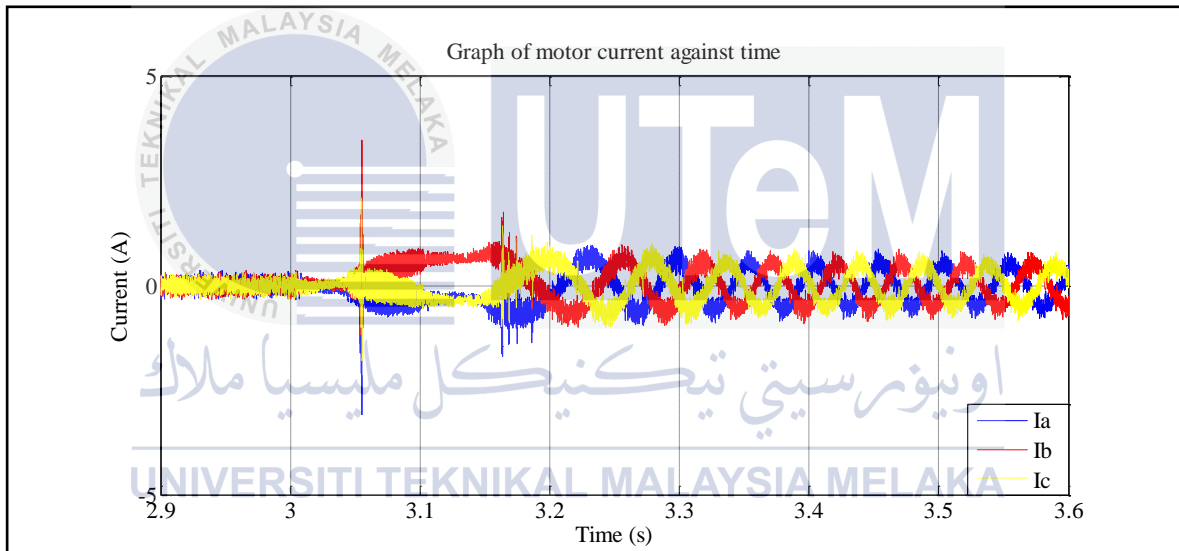


Figure 4.35: Zoom view during the starting current at load disturbance

For the phase current I_a , I_b and I_c in Figure 4.35 shows at a load disturbance point, $t = 3$ seconds, current become higher due to load torque occurred. The system become stable at $t = 3.3$ seconds. The current increase in 71% from no load condition rated. In low rated speed condition, current at a starting point and direction change point of a motor is represented lower than full and half rated speed condition.

Table 4.2 and 4.3 shows the results of this simulation to ease the analysis process.

Table 4.2: Simulation result of reference speed with step-up response

Reference Speed (rad/s)	Overshoot(%)	Undershoot (%)	Settling Time (s)	Rise Time (s)
209	7	0	0.48	0.12
105	16	25	0.5	0.09
31	60	67	0.62	0.07

Table 4.3: Simulation result of reference speed with load disturbance

Reference Speed (rad/s)	Undershoot (%)	Recovery Time (s)
209	69	3.6
105	57	3.5
31	55	3.4

4.5 Analysis

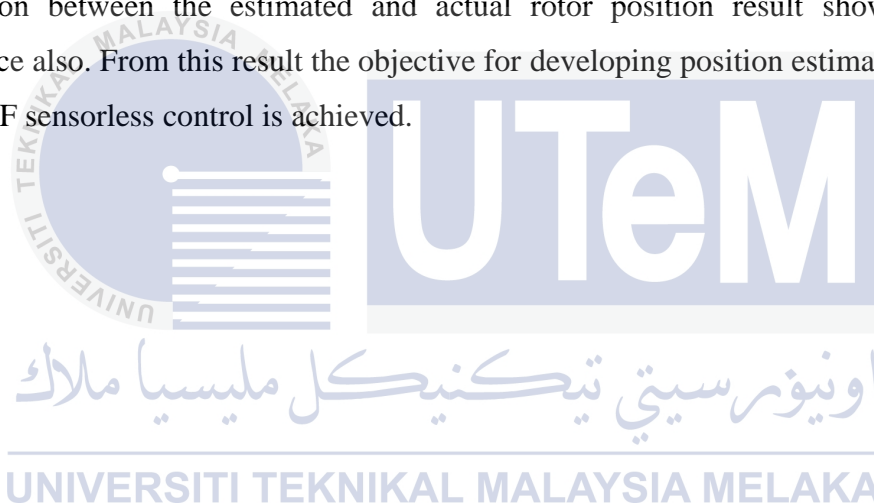
Various tests have been made in order to validate the proposed estimation algorithm. For this test some procedures or steps must be done to achieve the objective of this experiment. The step change in motor speed in full rated speed from 209 rad/s down to half rated which is 105 rad/s and then down again in lower speed which is 31 rad/s. After that, this step will perform again on sudden application of a 1 N.m load torque at $t = 3$ seconds while the motor run at full, half and low rated speed conditions.

In order to improve the strictness of these tests, the used of PI parameters in currents and speed control loops have been locked to the values tuned with the sensed version of the electrical drive. It is clear that a PI re-tuning, taking the presence of estimation into account, could reach a further improvement of the performance in sensorless control.

Figures in the result of speed measurement shows a comparison between the estimated speed and the measured speed for verification purpose of this simulation. From the result, it shows the ripple of the speed estimator is higher compared with the actual speed. It happens due to the stability of sensorless operation is affected by a momentary position error. A sensorless control loop cannot be designed to have a low bandwidth. Estimated and actual motor speed are in a good accordance. Furthermore, the estimated and actual motor speed shows a good performance in settling and rise time. But in estimated speed shows a high ripple at a starting and at $t = 5$ seconds due to change the direction rotation of the motor until it becomes in steady state. The estimator result at the full rated speed condition as shown in Figure 4.3 is the most stable compared with others speed values, which is half and low rated speed values as shown in Figure 4.9 and Figure 4.15. This is because the system is tuned at the full rated speed condition. From the observation, at this point the system is very stable. Furthermore, at a lower speed operation the system is unstable due to the sensorless low speed deficiency. Based on this condition, overshoot and undershoot will increased. This problem could be settled using self tuning, artificial intelligent controller such as Fuzzy Logic.

For the load disturbance test, it is really significant because the motor running under load condition and it can be observed during a transient operation. In Figure 4.21, 4.26 and 4.31 estimated speed measured are shown an abrupt ripple descending occurred when load torque is applied while the motor running. The load disturbance is applied at $t = 3$ seconds after the performance speed of the motor in steady state condition. The ripple is high when the load disturbance occurred due to the forced on their operation. This sensorless operation induces a transient oscillatory behavior in the motor speed. This occurs because during the start up the speed estimator begins its adaptation to a new operating point, and thus the estimated speed suffers from an oscillation. This test performed same as without load condition test in which the motor will running at 209 rad/s in full rated speed, 105 rad/s in half rated speed and lastly in 31 rad/s in low rated speed condition. In this reserch, the result is also same, which is the ripple occurred in the high speed range is lower than others speed ranges. Although some speed ripple appears in the sensorless condition of operation, the speed estimator remained stable during all trials. This can also be confirmed by the current pulses displayed during the sensorless operation.

Figure in the result of rotor position measurement show a comparison between the estimated and the measured one for verification purpose of this experiment. Found that, not much difference angle of the rotor position between actual and estimated results that tested. The difference between this tested can be observe which is the rotor position will increase in rad/s when the reference speed is higher. For the tested with load condition, the result shows have a curve at $t = 3$ seconds due to load disturbance occurred. The curve occurred during load disturbance is increasing when the rated speed of the motor is decreasing. This is because the system of the motor is more sensitive during lower rated speed and also be affected of the tuning process. The estimated and actual rotor position is measured without load and with load disturbance are shown while the motor running at 209 rad/s, 105 rad/s and 31 rad/s. Refer to the results, estimated and actual rotor position is in good accordance. When the load disturbance is applied during the motor running, the comparison between the estimated and actual rotor position result showed in good accordance also. From this result the objective for developing position estimation based on back-EMF sensorless control is achieved.



CHAPTER 5

CONCLUSION AND RECOMMENDATIONS

5.1 Conclusion

This project focuses on PMSM drive and the elimination of mechanical sensors without deteriorating the performances of that drive. The sensorless control has many advantages such as reduced hardware complexity, low cost and reduced size. Thus, the measured back-EMF of the machine is used to derive an estimation of the rotor position and speed for sensorless vector control. The sensorless PMSM drive is demonstrated to operate in a satisfactory manner with the presented method in wide speed range. The speed response is very good and the position error is measured to be insignificant.

In addition, a low time consuming sensorless control algorithm for PMSM for position and speed estimation was introduced, discussed and experimentally verified. The sensorless control system is based on the back-EMF space vector estimation. Other than that, the use of the back-EMF space vector is advantageous respect to any other system using flux estimation because of the integrator elimination avoiding the problem of integration drift that requires opportune devices or subsystems for its compensation. The proposed system in general is more reliable and cheaper than a complicated one without loss of performance respect to other control systems proposed in literature or in industrial applications.

In conclusion the proposed algorithm may be considered a very good alternative in terms of economy and precision without lack of performances and, furthermore exhibits an increase in reliability.

5.2 Recommendation

The simulation results show best expectations of the studied method in this thesis. However, the results in this thesis just from the simulation method and not in real time implementation work. Therefore, the experimental work implemented the back-EMF technique for PMSM is required to compare and analyzed the simulation and hardware results. The back-EMF techniques may also be reconfigured to estimate the parameters variation of the motor in real time.

Furthermore, the future works is on the back-EMF estimator algorithm. The research work required more parameters information to solve the problem at low speed condition. This is because the back-EMF signals at the low speed range are small. Besides that, the tuning process also will be required to solve this problem.

In addition, the future study should include the process on developing and simulating the method to capture the rotor position result which could be done in the MATLAB/SIMULINK software. This could be easy to observe and analyze the rotor position condition.

REFERENCES

- [1] J. Rais, and M. P. Donsión², “Permanent Magnet Synchronous Motors (PMSM) Parameters influence on the synchronization process of a PMSM”.
- [2] Matti Eskola, “Speed and Position Sensorless Control of Permanent Magnet Synchronous Motors in Matrix Converter and Voltage Source Converter Applications”, Tampere University of Technology 2006.
- [3] Zhong-ping Yang, Fei Lin, Qian Yuan and Hu Sun, “Sensorless Control of Permanent Magnet Synchronous Motor with Stator Flux Estimation”, Journal Of Computers, Vol. 8, No. 1, January 2013.
- [4] Enrique L. Carrillo Arroyo, Master Of Science In Electrical Engineering, “Modeling And Simulation Of Permanent Magnet Synchronous Motor Drive System”, University Of Puerto Rico Mayagüez Campus, 2006.
- [5] M. Aydin, "Axial Flux Mounted Permanent Magnet Disk Motors For Smooth Torque Traction Drive Application," in *Electrical and Computer Engineering*.
- [6] Erwan Simon, “Implementation of a Speed Field Oriented Control of 3-phase PMSM Motor”, *Digital Control Systems*, Digital Signal Processing Solutions, Application Report, 1999.
- [7] F. Genduso, R. Miceli, C. Rando, G. R. Galluzzo, “Back EMF Sensorless-Control Algorithm for High-Dynamic Performance PMSM,” IEEE Transactions on Industry Electronics, vol. 57, no. 6, pp.2092-2100, Jun. 2010.
- [8] J. Arellano-Padilla, C. Gerada, G. Asher, M. Sumner, “Inductance Characteristics of PMSMs and their Impact on Saliency-based Sensorless Control,” *14th International Conference of Power Electronics and Motion Control, EPE-PEMC 2010*.
- [9] Kalaigan, T.P. and T.S.R. Raja. Harmonic elimination by Shunt active filter using PI controller. In Computational Intelligence and Computing Research (ICCIC), 2010 IEEE International Conference on. 2010.

- [10] Hui, S. Y. and Chung, H. S., "A bi-directional AC-DC power converter with power factor correction," *IEEE Trans. Power Electron.*, vol. 15, no. 5, Sept. 2000, pp. 942-949.
- [11] Youness Aite driss, and Driss Yousfi, "PMSM Sensorless Control using Back-EMF Based Position and Speed Estimation Method".
- [12] Zihui Wang, Kaiyuan Lu, Yunyue Ye, Yong Jin, and Weiming Hong, "Analysis of Influence On Back-EMF Based Sensorless Control Of PMSM Due To Parameter Variations And Measurement Errors".
- [13] Fabio Genduso, Rosario Miceli, *IEEE*, Cosimo Rando and Giuseppe Ricco Galluzzo "Back-EMF Sensorless Control Algorithm for High Dynamics Performances PMSM", *IEEE Xplore* 2009.
- [14] M.P. Kazmierkowski, R. Krishnan, and F. Blaabjerg (2002). *Control in Power Electronics: Selected Problems*. San Diego: Academic Press. ISBN 978-0-12-402772-5.
- [15] D. C. Martins, L. C. Tomaselli, T. B. Lazzarin, and I. Barbi, "Drive for a symmetrical two-phase induction machine using vector modulation," *Inst. Electr. Eng. J. Trans. Ind. Appl.*, vol. 126, no. 7, pp. 835-840, 2006.
- [16] X.Yu, M.Dunnigan and B.Williams "A Novel Rotor Resistance Identification Method of an Indirect Rotor Flux Oriented Controlled Ind. Mach. System" *IEEE Tran. PE* vol. 17 no. 3, pp. 353-364, May. 2002
- [17] Hans-Petter Halvorsen "Introduction to Simulink" Telemark University College Department of Electrical Engineering, Information Technology and Cybernetics, 06. 06. 2011
- [18] Vasic, V., Vukosavic, S., and Levi, E.: 'A Stator Resistance Estimation Scheme for Speed Sensorless Rotor Flux Oriented Induction Motor Drives', *IEEE Trans. Energy Conv.*, 2003, 18, (4), pp. 476-483



